Applying a Template of Expected Uncertainties to Updating ^{239}Pu(n,f) Cross-section Covariances in the Neutron Data Standards Database

D. Neudecker[1], D.L Smith[2], F. Tovesson[1,3], R. Capote[4], M.C. White[1], N.S. Bowden[5], L. Snyder[5], A.D. Carlson[6], R.J. Casperson[5], V. Pronyaev[7], S. Sangiorgio[5], K.T. Schmitt[1], B. Seilhan[1], N. Walsh[1], and W. Younes[1]

[1]Los Alamos National Laboratory, Los Alamos, NM 87545, USA
[2]Argonne National Laboratory, Argonne, IL 60439-4842, USA (retired)
[3]National Nuclear Security Agency, Washington, DC 20585, USA
[4]International Atomic Energy Agency, P.O. Box 100, A-1400 Vienna, Austria
[5]Lawrence Livermore National Laboratory, Livermore, CA 94551-0808, USA
[6]National Institute of Standards and Technology, 100 Bureau Drive, Stop 8463, Gaithersburg, MD 20899-8463, USA
[7]International Atomic Energy Agency, P.O. Box 100, A-1400 Vienna, Austria (consultant)

August 22, 2020

DOI of formal publication: https://doi.org/10.1016/j.nds.2019.12.005

Abstract

Templates of uncertainties expected in specific measurement types were recently developed. One aim of these templates is to help evaluators in identifying (1) missing or suspiciously low uncertainties and (2) missing correlations between uncertainties of the same and different experiments, when estimating covariances for experimental data employed in their evaluations. These templates also provide realistic estimates of standard deviations and correlations for a particular uncertainty source and measurement type that can be used by evaluators in situations where they are not supplied by the experimenters. This information allows for a more comprehensive uncertainty analysis across all measurements considered in an evaluation and, thus, more realistic evaluated covariances. Here, we extend a template that is applicable to uncertainties expected in neutron-induced fission, (n,f), cross-section measurements. It is applied to improving covariances of ^{239}Pu(n,f) cross-section measurements in the database underlying the Neutron Data Standards evaluations. This particular example was chosen since this evaluation is primarily based on experimental information. Also, some uncertainties of individual ^{239}Pu(n,f) cross-section experiments in this database were suspected to be underestimated. The evaluated uncertainties obtained after updating the covariances in the database by means of the template indeed do increase compared to their original values. Even more importantly, the evaluated mean values change noticeably. These modified cross sections impact application calculations significantly, as is demonstrated by employing them in simulations of the effective neutron multiplication factor for a few selected critical assemblies. However, this updated evaluated ^{239}Pu(n,f) cross section should not be interpreted as the final one that should replace values of the current Neutron Data Standards project. Evaluations for the Neutron Data Standards of the ^{239}Pu(n,f) cross section must be linked to many other observables included in the associated database, most notably to cross sections for ^{235}U(n,f), but also to those for ^{10}B(n,α), ^{6}Li(n,t), ^{238}U(n,f), and ^{238}U(n,γ), because of included measurements of the ^{239}Pu(n,f) cross section that appear as ratios to these reactions. Some of these other reactions are correlated to further observables in the database. Hence, updating uncertainties of data sets of any of these observables can potentially impact the ^{239}Pu(n,f) cross section. Uncertainties for all measurements of these linked physical observables have to be updated before a comprehensive evaluation of the ^{239}Pu(n,f) cross section and its corresponding uncertainties can be provided.

Contents

1 INTRODUCTION

A new version of the Neutron Data Standards (NDS) was recently published [1]. Many measurements of neutron observables (*e.g.*, of neutron-induced fission cross section, prompt fission neutron spectra) are measured relative to observables that are evaluated as part of the NDS project co-ordinated by the IAEA. The resulting ratio data are then converted to results for the observable of interest by multiplying them with the evaluated NDS data. Consequently, the NDS evaluated data influence the evaluations of many other observables in nuclear data libraries beyond the observables included within the NDS project itself. Hence, these evaluated data have a significant and broad impact on nuclear data libraries. The same is true for those evaluated uncertainties obtained as part of the NDS evaluations. These evaluated uncertainties are thus propagated to all ratio measurements that are pertinent to a NDS observable if these evaluated data are used for conversion from ratio values to actual cross sections for specific observables. Hence, accurate evaluated data and realistic uncertainties for all NDS data are of critical importance for all nuclear data libraries that involve these data, either explicitly or implicitly.

The evaluated uncertainties of many NDS observables (^{6}Li(n,t), ^{10}B(n,α), ^{235,238}U(n,f), ^{238}U(n,γ), ^{197}Au(n,γ), ^{1}H(n,n), C(n,n) and ^{239}Pu(n,f) cross sections among them) were increased significantly compared to the previous NDS release [2]. The unrecognized sources of uncertainties (USU) [3, 4] given in Table IX of Ref. [1] were introduced *a-posteriori*. This was done as an expedient measure to counter criticism that the originally evaluated standard deviations obtained by the GMAP code [6, 5, 7] (which is employed in performing many NDS evaluations) were unrealistically small [2]. They were suspected to be unrealistically small because of:

(a) Missing or underestimated uncertainties of single experimental data sets in the GMA database underlying the NDS evaluations,

(b) Missing or underestimated correlations between uncertainties of the same and different experiments, and

(c) Missing unrecognized sources of uncertainties across many different experiments using the same technique.

Subsequently, it was shown [8] that the evaluated mean values are expected to change for multi-dimensional nuclear data (*i.e.*, more than one nuclear data value is calculated) if USU are introduced as a separate experimental uncertainty source for all measurements using the same technique. This can be easily understood by considering that adding an uncertainty component to one or more of the input data sets changes the weightings of data sets with respect to each other. A least-squares evaluation with a revised covariance matrix will lead to changes in evaluated mean values as well as their uncertainties. However, the recent NDS evaluation modified only the evaluated covariances but not the mean values. As mentioned above, this was done for expediency. But it is now known that this is not a statistically correct approach. Since this procedure is known to be incorrect for an evaluation of more than one observable, an investigation of the nature of USU contributions and how they should be applied to NDS evaluations is underway [4]. Furthermore, efforts are also ongoing to minimize the need for estimating USU contributions since it can be argued that they inherently subjective in nature and their inclusion should be an option of last resort.

One way to address points (a) and (b), and thus minimize the need for USU, is to compare the uncertainties available for a particular data set in GMA (GMA is the name of the database, while GMAP is the name of the

code employed for NDS evaluations) to typical uncertainties expected to be encountered in a specific measurement type. In order to streamline this process, templates of expected uncertainties and correlations that are tailored to particular measurement types have been developed [10, 11, 12, 9]. These templates help evaluators in addressing point (a) by checking for each experiment included in the evaluation whether all relevant uncertainty sources are taken into consideration, and if the uncertainty values and correlations are reasonable in magnitude. If some components are seen to be missing, and no specific objective information can be found elsewhere to fill the gaps, the template can provide estimates of these uncertainties and/ or correlations that are consistent across all measurements of this type, based on the best judgment of experts who are knowledgeable in these areas of experimental practice. If unrealistically low uncertainties are provided by experimenters compared to the template values, one should investigate whether these values are justified due to favorable set-up conditions or considerable effort undertaken to reach this precision. If no clues are found that support these low uncertainties as being realistic, they can be increased to the template value at the discretion of the evaluator who then has the responsibility of reporting this decision in documentation for the evaluation. However, it should be stressed again, that the template should be used ONLY to fill the gaps in the uncertainty analysis that cannot be addressed by carefully scrutinizing the literature relevant for that measurement.

The templates were also designed for experimenters, EXFOR compilers and editors of journal articles as a check lists to determine if typically expected uncertainties are provided for a new experiment. This might minimize the need to estimate missing uncertainties for future measurements.

Point (b) is difficult to address consistently across all data entering into an evaluation, as experimentalists rarely provide correlation information for their uncertainties, and they are even less likely to do so for uncertainties between experiments. The templates [9, 12], however, provide estimates of these correlations as an option for addressing such widespread deficiencies.

Point (c) can only be tackled by either estimating the USU directly [4] or by undertaking new measurements of an observable of interest by means of a novel technique, *e.g.*, [13, 15, 14, 16]. However, as mentioned earlier, by resolving the issues raised in points (a) and (b), one minimizes the need for assigning USU.

Here, we apply a template of uncertainties typically appearing in neutron-induced fission cross-section measurements, (n,f), to generate a more realistic representation of the experimental ^{239}Pu(n,f) covariances in the GMA database. It should be highlighted that the ^{239}Pu(n,f) reaction is not formally defined as a standard but rather as a reference cross section within the NDS project. It is included within the set of reactions involved in the GMAP fitting process due to the large number of ratio measurements that involve the ^{239}Pu(n,f) cross section. As it is a reference reaction, its uncertainties are generally larger than for the (n,f) reaction standard, ^{235}U(n,f). So larger changes in the ^{239}Pu(n,f) cross sections are expected. For instance, differences up to 6–8% were observed from 15–20 MeV in the 2006 version [6] compared to its previous evaluation [17].

The template used is summarized and extended in Section 2 compared to its original form published in the conference proceeding in Ref. [9]. In Section 3, it is shown that, indeed, uncertainties and correlations within a particular experiment, and between different experiments, were missing for many individual ^{239}Pu(n,f) cross-section data sets in the GMA database. The resulting evaluated uncertainties presented in Section 4 are larger at most energies than those obtained before updating the experimental covariances. But, even more importantly, the evaluated mean values change when the revised covariances are used, for the reason mentioned above. It is shown that this difference in the evaluated data impacts the calculated neutron multiplication factor of fast critical assemblies significantly. Also, other cross sections (*e.g.*, ^{235}U(n,f)) are influenced through revision of the ^{239}Pu(n,f) covariances due to cross-correlations between uncertainties and ratio measurements of experiments of both observables. It is concluded in Section 5 that uncertainties of all measurements within the NDS database need to be updated for a comprehensive assessment of realistic uncertainties as well as the cross-section values themselves.

2 EXTENDED TEMPLATE OF UNCERTAINTIES FOR (N,F) CROSS SECTIONS

Several uncertainty sources that typically appear in (n,f) cross-section measurements where fission fragments are detected are listed in Table 1. These uncertainty sources encountered in (n,f) measurements stem from: Determining the sample mass, δN, counting statistics, δc, correcting neutron attenuation, $\delta\beta$, multiple scattering, δm, determining detector efficiency, $\delta\varepsilon$, correcting for fission-fragment angular distribution, $\delta\alpha$, background, δb, determining energy, δE, neutron flux, $\delta\phi$, sample impurity, $\delta\zeta$, and deadtime, δd. The realistic ranges of uncertainties for some of these sources depend on the details of the set-up. Typical (n,f) measurements were categorized in six broad classes in Ref. [9] allowing us to give more targeted and realistic estimates for individual uncertainty sources. They are summarized here briefly to clarify the nomenclature convention within this manuscript:

- Absolute (n,f) measurements: The (n,f) cross section is measured directly by detecting fission fragments. The neutron flux, ϕ, detector efficiency, ε, and number of atoms in the sample, N_1, have to be quantified explicitly for this measurement type.
- Shape (n,f) measurements: The shape of the (n,f) cross section as a function of incident neutron energy, E, is given, while the normalization factor of the (n,f) cross section is not quantified. N_1 and the normalization of ϕ and ε are not determined, while the energy dependence of ϕ and ε need to be given. For a white neutron source, this normalization of ϕ is fixed. However, one needs to measure its relative intensity for mono-energetic beams at several E.
- Absolute clean ratio measurement: The (n,f) cross section is determined as a ratio to a reference reaction. The latter is measured with the *same or a very similar* fission fragment detector in the same or very similar set-up. In this arrangement, determining ε and ϕ reduces to quantifying the differences that arise in these measurements due to those inherent between properties of the element/ isotope in question and the reference element/ isotope. The associated correction is usually small. The numbers of atoms in the sample have to be quantified for both isotopes.
- Shape clean ratio measurements: These measurements differ from absolute clean ratio ones only in that the normalization of the ratio (n,f) data is not quantified.
- Absolute indirect ratio measurements: The (n,f) cross section is measured as a ratio to a reference reaction with two or more *different* detectors. Consequently, efficiencies for all detectors need to be quantified along with the number of atoms in the samples. Determining ϕ reduces to a small correction factor similarly to clean ratio measurements.
- Shape indirect ratio measurements: These measurements differ from absolute indirect ratio ones only in that the normalization of the ratio of (n,f) cross sections is not quantified.

The (n,f) cross section can also be provided by experiments that measure the prompt neutrons emitted after fission. This type of experiment differs from those detecting fission fragments in that it depends on the accuracy of the average prompt neutron multiplicity and the angular distribution of the neutrons emitted after fission—thus adding two more uncertainty sources. The background in an (n,f) measurement that involves detecting neutrons is also different from one that counts fission fragments. In addition, these experiments require distinctly thicker sample targets, thereby, increasing the effect of neutron multiple scattering compared to using thin samples. Hence, overall larger multiple scattering and background uncertainties are expected. One example of this measurement type is the experiment by Gayther [18].

Yet another method to determine the (n,f) cross section is to measure the fission product yields as presented in Section III.D of Ref. [19]. The fission products are measured using radio-chemistry, gamma spectrometry or a combination of both. The (n,f) cross sections are then estimated by using assumed values for fission product yields. A major uncertainty source is, thus, the fission product yield uncertainty. Hence, the most abundant, and therefore presumably the best known, fission products are usually used (*e.g.*, fission yields of ^{129}I or ^{137}Cs isotopes).

The importance of these two different measurement techniques lies in discovering previously unknown systematic uncertainties in the standard approach (measuring fission fragments). However, not a single ^{239}Pu(n,f) cross-section data set appears in the GMA database that was undertaken by measuring fission product yields. Only one exists where fission neutrons were detected [18]. For this reason, no detailed template of uncertainties is being established for these measurement approaches.

In the subsections below, the modifications in the current template, compared to the earlier version, are summarized. It cannot be overstressed to readers of this paper that the recommended numbers and correlation coefficients in Tables 1 and 2 should be used as a last resort only if no other realistic value can be estimated either from the literature related to a particular experiment or by discussion with its authors.

2.1 Sample Mass Uncertainty δN

The following uncertainties might be encountered in δN: An uncertainty in (a) determining the number of atoms in the sample, (b) correcting for non-uniform samples, and (c) correcting for a non-uniform neutron beam. If at least one of the two, sample or beam, is uniform in the area of the sample illuminated by the beam, uncertainties (b) and (c) will not be an issue.

For analyzing $\delta N_{(b\&c)}$, one needs to also take into account whether only part or all of the sample is illuminated by the neutron-beam [21]. If the beam is smaller than the target and the target is uniform, with the beam in the center

Table 1: Typical uncertainty sources encountered in (n,f) measurements that involve detecting fission fragments are listed, including proposed realistic ranges of uncertainties and shapes of correlations if missing for a specific measurement. The modifications from the preliminary version of the template in Ref. [9] are highlighted in red. The energy uncertainties δE are understood to encompass energy calibration and time resolution.

Unc. source	Typical range	Cor(Exp$_i$,Exp$_i$)	Cor(Exp$_i$, Exp$_j$) $i \neq j$
$\delta N_{(a)}$	$> 1\%$	Full	$\neq 0$ if same technique/sample
$\delta N_{(b\&c)}$	0-0.5% (Vapor-deposited target)	Full	$\neq 0$ if same technique/sample
	1% (Painted/electro-plated target)	Full	$\neq 0$ if same technique/sample
δc	Eqs. (3) and (5)	Diagonal	0
$\delta\beta$ & δm; δm	0.02–2%	Gaussian [20]	0.5–0.75
$\delta\beta$ & δm; $\delta\beta$	0.2–1%	Gaussian	0.5–0.75
$\delta\varepsilon$ & $\delta\alpha$; $\delta\varepsilon$	1.1-4%	Close to full	0.5–1
$\delta\varepsilon$ & $\delta\alpha$; $\delta\alpha$	Compare to nuclear data	Gaussian	0.75–1.0
δb	0.2–>10%	Gaussian	Possible
δE	1%, 1–3 ns (TOF, for given TOF length)	From conversion	Technique-dependent
$\delta\phi$	0%, >1%	0.5–Full	Technique-dependent
$\delta\zeta$	See Table 3	0.9–1	0.5–0.75
δd	>0.1%	Full	0

Table 2: Typical uncertainty sources encountered in (n,f) measurements that involve detecting fission fragments are listed dependent on their specific measurement type. The amendments from the preliminary version of the template in Ref. [9] are highlighted in red.

Unc. source	Absolute	Absolute clean ratio	Absolute indirect ratio
$\delta N_{(a/b\&c)}$	See Table 1	Both samples	Both samples
δc	Eqs. (3) and (5)	Both, combined	Both, combined
$\delta\beta$ & δm; δm	0.2–2%	0.02–0.2%	0.2–2%
$\delta\beta$ & δm; $\delta\beta$	0.2–1%	Less than absolute	0.2–1%
$\delta\varepsilon$ & $\delta\alpha$; $\delta\varepsilon$	1.1–4%	0.3–4%	1.1-4%, 0.5–1%
$\delta\varepsilon$ & $\delta\alpha$; $\delta\alpha$	Compare to nuclear data	Compare to nuclear data	Compare to nuclear data
δb	0.2–>10%	0.2–>10%	0.2–>10%
δE	1%, 1-3 ns	Combined	Both detectors
$\delta\phi$	>1%	Cancels or small	Cancels or small
$\delta\zeta$	See Table 3	See Table 3	See Table 3
δd	>0.1%	Both combined	Both detectors

or *vice versa*, the non-uniformity correction is not needed. In this case, δN only accounts for quantifying the number of atoms in the sample, $\delta N_{(a)}$.

However, a large beam does not necessarily guarantee a uniform beam. It might just reduce its non-uniformity. Thus, it is essential that uniformity of beam and samples be validated in all measurements.

If sample and beam are non-uniform in the area of overlap, $\delta N_{(b\&c)}$ might apply. Its absolute magnitude depends on the non-uniformity of beam and target fabrication. In general, vapor-deposited targets tend to be more uniform, leading to a low $\delta N_{(b\&c)}$ on the level of 0.0–0.5 %, if large beam spots are also used. Electroplated and painted targets are often more significantly non-uniform. Then, corrections should be applied to mitigate resulting effects on the cross section. For a large non-uniformity, *e.g.*, 2:1 contrast ratio across beam or target, corrections may amount to a few percent. Here, we estimate that $\delta N_{(b\&c)}$ is $\approx$ 20 % of its correction, thereby leading to a value of up to 1%. This conservative estimate is recommended if $\delta N_{(b\&c)}$ is not specified in the literature, but a correction for the effect was applied. If no correction was applied, and there is reason to suspect large non-uniformities of sample and beam, an additional uncertainty of a few percent (perhaps as high as 5 %) might apply. This uncertainty would not necessarily be constant, but would likely be energy-dependent, as the beam shape, and hence the correction, changes with incident neutron energy.

The uncertainty in determining the number of atoms in the sample, $\delta N_{(a)}$, is maintained from Ref. [9]. It is technically possible to achieve $\delta N_{(a)}$ values lower than 1% in dedicated measurements, but 1% is a realistic conservative estimate if nothing else is given.

Table 3: Typical ranges of sample-mass impurity uncertainties, $\delta\zeta$, are provided for ^{239}Pu and ^{235}U samples, dependent on the isotopic content of the main isotope. It is assumed that the contaminants are of the same element as the isotope investigated. These numbers are understood as a guideline if no $\delta\zeta$ values are given in the literature but the sample contamination is explicitly stated.

Isotope content (%)	$\delta\zeta(^{239}\text{Pu})$ (%)	$\delta\zeta(^{235}\text{U})$ (%)
100	0	0
99.5	0.05	0.075
99.0	0.1	0.15
97	0.3	0.4
95	0.5	0.6

If several samples are used, the non-uniformity of, and the number of atoms in, each sample have to be determined, and this will lead to increased δN. This could apply to measurements with a stack of samples of the same isotope or measurements as ratios to a monitor reaction.

The non-uniformity of the neutron beam could potentially cancel if the cross sections were measured as a ratio to a monitor provided that these samples had the same non-uniformity and were irradiated simultaneously in the same neutron beam. However, it is unlikely that two samples would have similar non-uniformity. Of course, there could be a partial cancellation, or an enhancement depending on the details of the non-uniformity (*i.e.*,the nature of the spatial distribution of sample atoms) and the relative orientation of these two targets. A diverging orientation of the non-uniformity of the targets would lead to distinct corrections for these targets.

Many ratio ^{239}Pu(n,f) data sets in the GMA database involve the ^{235}U(n,f) reaction. If they are absolute data, $\delta N_{(a)}$ needs also to be determined for the ^{235}U sample. In general, it is harder to measure the number of atoms in ^{235}U rather than ^{239}Pu samples because:

- There are several contaminants in ^{235}U (*e.g.*, those of ^{233,234,236}U) that are difficult to resolve with α-spectroscopy from ^{235}U as they have relatively short half-lives and nearby α-energies.
- Mass spectrometry on uranium material is difficult to perform to high precision because of its ubiquity compared to plutonium. ^{239}Pu, on the other hand, typically has ^{240}Pu contaminations which cannot be resolved by α-spectroscopy but is easily measured by mass spectrometry.
- The half-life of ^{239}Pu is much shorter than that of ^{235}U, so the needed count time is reduced for the former.
- Also, when measuring ^{235}U and ^{239}Pu fission ratios, additional difficulties might arise due to the different α-emission rates of those two isotopes. For a geometry that is effective for measuring ^{235}U, ^{239}Pu can have an extremely high α-emission rate leading to pile-up issues. This problem can be avoided with the right experimental configuration.

Consequently, it is expected that $\delta N_{(a)}$ is usually slightly higher for ^{235}U than for ^{239}Pu samples. If this trend is specified to be different in particular measurements, one should investigate why this might be the case.

The sample mass uncertainty δN leads, in general, to a fully correlated uncertainty source that applies to all incident neutron energies of the same experiment. One exceptional case would be if different samples were used to measure the (n,f) cross section at specific incident neutron energies. Another reason could be that an apparent non-uniformity of sample and beam was not corrected for and the beam varies with E. Then, so does $\delta N_{(b\&c)}$ thus leading to a strong but not full correlation. As we expect these two cases to be exceptions rather than the rule, we recommend to use a full correlation, in general, for $\delta N_{(b\&c)}$ in Table 1.

Correlations between δN of different experiments can arise if the same sample was used. This might seem that it should be a rare occurrence because few cases are explicitly documented. However, this seems to be more common than the literature suggests. For instance, the sample used by Lisowski *et al.* [23], was re-used by Tovesson *et al.* [24] and Staples *et al.* [25] according to private communication with F. Tovesson. In addition, P.W. Lisowski received samples from D.L. Smith (which are documented in Ref. [26]. So, they also were used in experiments by J.W. Meadows who worked in the same laboratory as D.L. Smith) and A.D. Carlson after fission measurement campaigns at their respective institutes were terminated. D.L. Smith also sent some samples to NIST (A.D. Carlson) which were sent on later to LANL and LLNL. Hence, it is highly likely that samples were shared between more experiments in the US than explicitly documented. Contamination and sample size information might provide some hints if the same samples were re-used.

Even if different samples were employed, only a handful of measurement techniques were used to determine N for ^{239}Pu(n,f) cross-section data in GMA (α-counting, direct weighing and the threshold method). This leads to correlations between $\delta N_{(a)}$ for different measurements. For instance, α-counting was used frequently to determine the sample mass [32, 27, 43, 38, 34, 33, 41, 36, 28, 39, 42, 29, 30, 31, 23, 37, 35, 40]. According to Ref. [45, 44], an α-counting measurement is at best precise to 0.1% which would be the common uncertainty across all the measurements employing this approach. In older measurements and those not dedicated to achieve high precision, the uncertainty might easily be higher and hence the correlations between sample mass uncertainties of different experiments might be non-negligible, and a correlation of up to 0.5 might be a reasonable value to apply to $\delta N_{(a)}$.

2.2 Counting Statistics Uncertainty δc

In the original template, it was recommended that if δc is not provided, one could add statistical uncertainties of a similar magnitude on average compared with δc of other measurements with the same isotopes, in the same energy range and with a similar binning size, *e.g.*, for white neutron source experiments. This procedure is arbitrary insofar as it does not take into account the count acquisition time, the amount of material in the target and the intensity of the neutron beam. Two different methods to estimate δc are proposed below:

2.2.0.1 Estimating δc from acquisition time, neutron flux and number of atoms in the sample The cross-section counts $C(E)$ dependent on E are given as:

$$C(E) = tN_1 \int_E \sigma(E)\phi(E)\mathrm{d}E, \tag{1}$$

with the acquisition time, t, the number of atoms in the sample, N_1, the cross section to be measured, σ, and the neutron flux, ϕ. This equation is simplified since it does not take into account effects such as background correction, correction for impurities in the sample, etc.

The statistical uncertainty can be approximated by

$$\delta c \approx \frac{\sqrt{C}}{C} \tag{2}$$

using t, N_1 and ϕ for absolute or shape data. For ratio measurements, where N_1/N_m is measured with subscript "m" for the monitor isotope, δc is given by:

$$\delta c \approx \sqrt{\delta c_m^2 + \delta c_1^2}. \tag{3}$$

If t, N_x and ϕ are missing, one has to make educated guesses concerning these observables based on similar measurements of the research group or at the same facility. These educated guesses might introduce biases. For instance, even if the neutron flux is given for a specific facility in another journal article than the one describing the actual experiment, not necessarily the same neutron-producing target, collimators, etc., might have been used for the measurement of the quantity of interest. Also, t might be hard to estimate if the duration of the measurement is not known. This is yet another example that shows how important it is that key information about a measurement is recorded either in journal publications (if space permits) or laboratory reports, in order to make the most use of the data without introducing bias into an evaluation.

2.2.0.2 Estimating δc from the spread of the experimental data The above method requires a lot of information which might render it unfeasible. Another approach looks at several experimental values in energy ranges where the data are expected to be flat or at least not widely varying within a short energy range (*e.g.*, resonances). The variation of the experimental data, δv, *i.e.*,

$$\delta v = \frac{1}{\langle\sigma_i\rangle}\sqrt{\frac{1}{M}\sum_{j=1}^{M}(\sigma_{i,j} - \langle\sigma_i\rangle)^2}, \tag{4}$$

with

$$\langle\sigma_i\rangle = \frac{1}{M}\sum_{j=1}^{M}\sigma_{i,j}, \tag{5}$$

could be used as an upper bound of the statistical uncertainties δc. This procedure implicitly assumes that the fluctuations in several experimental data sets only stem from the statistical spread of data. It disregards fluctuations between data sets due to various systematic effects, and therefore it likely overestimates δc.

In ratio measurements, fission fragment counts are recorded for both samples independently even if they are measured at the same time within the same detector. However, δc is expected to be given in a combined fashion for all ratio measurements as the ratio data themselves are reported as combined quantities. Of course, it would be best practice if the experimenter not only provides δc directly but also clearly states whether it is for one isotope or for the ratio data. In general, δc is expected to have a diagonal correlation matrix.

2.3 Attenuation and Multiple Scattering Uncertainties $\delta\beta$ and δm

Because thin samples are usually utilized in (n,f) cross-section measurements, the neutron attenuation and multiple scattering corrections are generally attributable to the influence of the surrounding material on the incident neutron energy. However, if thick samples are employed, scattering in the samples needs also to be quantified (*e.g.*, when measuring the (n,f) cross section via detecting prompt neutrons rather than fission fragments).

Neutron attenuation is understood as the loss of incident neutrons in the structural material before reaching the sample. Multiple scattering refers to the fact that some incident neutrons down-scatter in energy before hitting the sample. This results in incident neutrons of lower energy than expected and thus an assignment of fission-fragment counts to the wrong energy bin, *e.g.*, in white neutron source experiments. Both of these effects are usually corrected in a combined manner in contemporary measurements. In past measurements they were often determined separately using various approximations. To emphasize that point, attenuation and multiple scattering uncertainties are re-grouped in the template in Tables 1 and 2 into combined entries but the actual uncertainties and correlation coefficients are supplied separately. These values are carried over from the original template [9]. More general information is given below on how these effects were corrected.

The neutron flux is measured event-by-event prior to the neutrons impinging on the fission chamber in absolute experiments that use the associated particle method. The neutron production rate is measured directly at the neutron source by detecting the charged particle that is associated with the neutron-producing reaction. Attenuation and multiple scattering of neutrons between the neutron-producing target and fission sample needs to be corrected, accounting for the neutron beam (profile, energy spread, etc.), room configuration, target and backing material. In clean-ratio measurements, only neutrons attenuated and multiply scattered between the two targets have to be considered and, hence, the correction is smallest for clean ratio measurements. This factor is larger for indirect than for clean-ratio measurements, as usually more attenuating material is situated between the two samples.

Attenuation and multiple scattering effects are often calculated by Monte Carlo neutron transport codes such as MCNP [46]. The contributing sources to $\delta\beta$ and δm are then the uncertainties in Monte Carlo statistics, geometrical accuracy of the input deck, and in the nuclear data and physics models underlying the simulations. One should keep in mind for the latter two contributions that even small constituents with large cross section could play a role, especially in the resonance range. Attenuation also depends to a lesser extent on the target thickness, the backing material and its thickness. Attenuation and multiple scattering were more difficult to simulate more than 20 years ago as neutron transport codes were not as sophisticated as today and some calculations might not have been feasible due to the computational cost.

2.4 Detector Efficiency and Fission-Fragment Angular Distribution Uncertainties $\delta\varepsilon$ and $\delta\alpha$

In the original template [9], the detector efficiency and fission-fragment angular-distribution correction uncertainties, $\delta\varepsilon$ and $\delta\alpha$, were listed as two separate uncertainty sources. However, the fission-fragment angular-distribution correction should be an inherent part of the detector efficiency [47], indicated as a change in Tables 1 and 2. If experimentalists give a separate uncertainty component for the fission-fragment angular-distribution correction, there were approximations made in this term which leads to increased $\delta\alpha$.

In general, the efficiency is a function of E and depends on:

- The anisotropy of the fission fragments which is an effect caused by:
  1. The inherent anisotropies of fission-fragment emission for the specific isotopes measured.
  2. The kinematic boost of the fission fragments occurs in the direction of the incoming neutron beam, and it reflects the momentum transfered by the neutron to the fragments.
- The magnitude of the stopping power affecting emission of fission fragments from the foils. Knowing it accurately is especially important for thin backings where the fission fragments must pass through the backing before being detected.

- The roughness (irregularity) of the sample surface. The rougher a sample is, the fewer fission fragments are emitted from the sample for a given average surface thickness.
- The material of the sample backing.
- On the specific event region selected for the particle-identification signals, if applicable.

Below, each uncertainty source is described in detail separately.

The kinematic boost of fission fragments is fairly well-understood for E = 10–20 MeV from relativistic or non-relativistic two-body kinematics [47]. However, for $E > 30$ MeV there are basically no measured data to guide its trend, and full kinematic momentum transfer might no longer be guaranteed [50]. This might affect experiments above 30 MeV. It is present in absolute or shape measurements, and it persists for indirect ratio measurements if the monitor isotope is non-fissile. This effect is expected to be the same for two different fissile targets and it cancels for clean ratio measurements using two targets of the same thickness with both deposits facing in the same direction. Hence, no uncertainty applies for this specific case. In a clean ratio measurement, where the sample of interest and the monitor sample are aligned in a back-to-back configuration, one needs to correct for the difference in the angular distribution of the fission fragments due to their distinct kinematic forward-boost. In old measurements, experimentalists would account for this effect by rotating the fission chamber by 180 degrees such that the samples are again back-to-back, but in opposite orientation with regard to which sample faces the neutron source. The results of both measurements are then averaged, implicitly averaging over the kinematic boost of the fission fragments. If this effect behaves non-linearly a small correction would nevertheless be required. If no correction was applied for the angular distribution of fission fragments due to the kinematic boost, or the fission chamber was not rotated, then the kinematic boost effect could introduce a bias in the measured cross section at medium energies and above. A crude estimate of this effect would be 3–4%, but the magnitude would depend on the cos(theta) acceptance and target thickness. If one employs very flat targets and a high-efficiency fission chamber, this effect might be negligible at low energies, but would be still noticeable for $E > 1$ MeV. One could expect the effect to be of the order of 1% and be primarily caused by the anisotropy of the fission fragments.

The inherent anisotropy of fission-fragment emission depends on the isotopes measured. Therefore, it does not cancel in any type of measurement. The effect might be smaller for clean ratio measurements than absolute/ shape or indirect ratio measurements if the anisotropy of fission-fragment emission is similar for the actinide in question and the monitor isotope. They usually differ most at those energies where first- or multiple-chance fission channels open, especially, if these threshold energies do not coincide for the isotope in question and the monitor one (see Fig. 2 of Ref. [48] or Ref. [49]). For instance, if one compares the fission-fragment anisotropy of ^{235}U and ^{238}U (see, *e.g.*, Figs. 5.12 and 5.13 in Ref. [50]), it is obvious that not only the absolute magnitude but also the shapes as a function of E deviate—especially, at the threshold of the ^{238}U(n,f) cross section and second- and third-chance fission threshold of ^{235,238}U(n,f) cross sections. To estimate the magnitude of the effect and the energy, E, where it is relevant, one could examine the inherent angular distribution of fission fragments, deduced either from measurements, nuclear data, if available, or nuclear theory calculations [51]. This recommendation to look at available information on $\delta\alpha$ is summarized in Tables 1 and 2 by "Compare to nuclear data". The magnitude of the effect depends specifically on the experiment, as one needs to include angle and energy acceptance limits of the detector in any analysis designed to study the effect. The same reasoning should apply to investigating these effects for stacks of targets.

Especially at shallow exit angles of the fission fragments from the foil, stopping power affects the fission fragments through scattering and energy degradation, and this effect would be observed at all energies [52, 53]. The stopping power effect is contingent on the thickness and isotopes of the foils. This effect is often calculated by programs such as SRIM, TRIM, GEANT [54, 55, 56]. Internal to these codes, stopping power data are incorporated in a manner which can lead to correlations between the results of analyses of these experiments. In old measurements instead, it was common practice to employ samples that were as thin as possible to minimize the effect. To estimate its impact on ε, one could assume that an effective efficiency, ε, approaching 99.5% could be achieved, and that the 0.5% loss is completely attributed to the effect of stopping power [57]. If two targets of different thicknesses were used for ratio measurement, the stopping power would depend on the difference in the thicknesses of the targets, and the bounding value would be the fraction of events that did not escape the target. A crude guess of that difference might be 1%. The uncertainty would be based on whether or not a correction was applied for the effect. Also, samples with more than 100 mg/cm^2 effective thickness would affect the efficiency due to a higher effect of stopping power.

Usually, as mentioned earlier, painted and electro-plated targets would be subject to considerable roughness while vapor-deposited targets have little roughness. The roughness of the samples leads to an energy-dependent correction factor.

The amount and material of target backing used could affect the efficiency due to neutron multiple scattering and back-scattering effects. Back-scattering effects might require corrections up to 1%, but they might cancel in ratio

measurements if the same target backings are used. Carbon backings could be problematic because they often have large ripples that add to roughness. If foils are backed by rough carbon materials, the detector efficiency can be impacted by as much as ≈10%, as can be seen in Fig. 15 of [16]. High-Z material backing (for instance, platinum) could potentially affect the fission fragments [52, 58] if Coulomb scattering is not handled properly.

All these contributions to ε are of similar importance. The fission-fragment angular distribution correction due to the forward-boost effect is non-negligible at high E. The correction due to the inherent angular distribution of fission fragments matters most at first- and multiple-chance fission thresholds. This latter contribution leads clearly to an E-dependent detector efficiency rather than the constant detector efficiency assumed in the template for $E < 10$ MeV. The stopping power correction applies to all E.

The uncertainties due to corrections of roughness, stopping power and angular distributions of fission fragments due to the kinematic boost can be assumed to be very strongly, if not fully, correlated. The correlation matrix for the uncertainties stemming from the correction due to the inherent angular distribution of the fission fragments depends on the correlation matrix of the angular distribution data used for the correction. Hence, the correlation matrix for ε can be assumed to be strongly correlated except in energy ranges where the uncertainty due to the inherent angular distribution of fission-fragment emission dominates $\delta\varepsilon$.

The proposed correlation coefficient values for $\delta\varepsilon$ and $\delta\alpha$ between different experiments were carried over from Ref. [9]. The range of correlations for $\delta\varepsilon$ varies widely between 0.5 and 1 because it depends on whether the measurements investigated are absolute, clean ratio, or indirect ratio measurements, and whether the same/ similar assumptions underlay the detector efficiency determination of two different measurements. The same or similar assumptions could potentially apply to estimating uncertainties related to determining the fission-fragment angular distribution due to kinematic forward boost, roughness and stopping power as they are simulated or corrected using the same equations or data throughout many measurements.

For indirect ratio measurements relative to a physical observable other than (n,f) (*e.g.*, ^{10}B(n,α)), correlations between the uncertainties of both detectors need to be estimated. Correlations between non-(n,f) and fission chambers are zero as the effects of stopping power of fission fragments in the samples and inherent angular distribution of fission fragment obviously do not appear for the former type of measurements. However, non-zero correlations between $\delta\varepsilon$ of the reference measurements can appear between two measurements if similar detector types are employed.

2.5 Sample Impurity Uncertainties $\delta\zeta$

Corrections for sample impurities are accomplished by using the actual magnitude of the measured contamination and the nuclear data for the (n,f) cross section of the contaminating isotopes. Nuclear data uncertainties for the (n,f) cross section of the contaminating isotopes can be retrieved by knowing which nuclear data were employed for the correction or by guessing at the nuclear data used according to the time and location of the measurement. The uncertainty in the measured contaminant depends strongly on its actual level. If $\delta\zeta$ is not provided for an experiment, but, impurities are explicitly stated and were corrected, one can use for ^{239}Pu and ^{235}U samples the estimates of $\delta\zeta$ in Table 3. If no reference is made to whether a correction for contaminations has been undertaken, one could assume the level of contamination as an uncertainty, and that could be rather large for some experimental data sets. The correlation information from Ref. [9] was carried over to Table 1 unchanged.

3 UPDATING ^{239}Pu(n,f) COVARIANCES IN THE NDS DATABASE

All ^{239}Pu(n,f) experimental covariances in the GMA database were revised following a multi-step procedure:

1. A detailed literature review was undertaken for each measurement. The respective EXFOR entry [59], GMA entry description [5, 1, 2] and literature associated with each data set were consulted to extract relevant uncertainty information for the data set. It is highlighted in Table 4 that in many cases additional uncertainties could be added. It should be emphasized that this step is well-supported by the information actually supplied by the experimentalist of the particular data set.

2. All uncertainty sources found in EXFOR, GMA or the literature are then compared to those in the template. If one or more items are completely missing, clues in the literature are investigated to estimate them with the help of the template. For instance, if $\delta\zeta$ is missing but a sample contamination is given, a better estimate for $\delta\zeta$ can be made. Another example is if it is mentioned that carefully designed low-mass experimental set ups were used for the measurement, then δm and $\delta\beta$ are assumed to be smaller than template values. If no information is provided, uncertainty values and correlations within the range of those recommended by the template are used. If standard deviations of specific uncertainty sources are suspiciously low compared to template values,

and there is no supporting evidence found in the literature to explain these values, they are increased following values in Table 4. Additional comments for specific data sets are provided in Table 5.

3. The GMA entry is then updated with the information from above using the code ARIADNE [83]. Outlying uncertainties, δo, are set to zero in this step. These were added in the previous NDS evaluation version [2] to clearly flag outlying experimental data points. δo is determined based on the difference between total experimental uncertainty and ratio of prior value to experimental data. When the experimental uncertainties are re-estimated, δo also have to be re-calculated.

4. δo uncertainty components are re-introduced into the GMA entry based on newly estimated total uncertainties of each individual data set. The procedure applied to the previous and current NDS evaluations was strictly followed, namely: δo is added if the difference, $d_p(E)$, of one absolute experimental value, $e(E)$, from the prior value, $p(E)$,
$$d_p^a(E) = 100|(1 - p(E)/e(E))|, \tag{6}$$
of the fourth GMAP iteration (at least two are needed for the Chiba-Smith approach to address Peelle's Pertinent Puzzle [6]) satisfies the following constraints:
$$\begin{aligned} &d_p^a(E) \geq 2\delta t_e(E) \quad \text{for a single outlying data point,} \\ &d_p^a(E) \geq \delta t_e(E) \quad \text{if the following data point of} \\ &\qquad\qquad \text{the same data set satisfies this constraint,} \end{aligned} \tag{7}$$
where $\delta t_e(E)$ is the total relative uncertainty of an individual experimental data point in % relative to $e(E)$. The outlying uncertainty of point $e(E)$ is then defined as
$$\delta o(E) = \sqrt{\left(d_p^a(E)\right)^2 - \left(\delta t_e(E)\right)^2}. \tag{8}$$
It is included as a separate GMA uncertainty into the GMA database with a medium range correlation component not correlated with any standard deviation for other data sets.

For shape data, the normalization, n_s, of this data set is evaluated within the code GMAP. This change in normalization of each data point $e(E)$ in this data set is accounted for in the δo-procedure by defining the difference to the prior as:
$$d_p^s(E) = 100|(n_s - p(E)/e(E))|, \tag{9}$$
and then applying Eqs. (7) and (8) with d_p^s instead of d_p^a. It is listed in Table 4 which data sets were updated with δo.

5. Correlations between uncertainties of different data sets were introduced. The code GMAP only allows constant correlation factors to be provided between partial uncertainties of two data sets. These were estimated following Table 2 in general and Table 6 specifically. Measurement information pertinent to separate physical sub-processes was identified in Table I of Ref. [84] for each measurement listed in Table 4. For instance, it was identified for each measurement which technique was used to measure ϕ or to estimate N_1. If two measurements used the same approach to estimate a sub-process of the measurement (*e.g.*, neutron flux, background, detector efficiency), the correlation factors listed in Table 6 were assigned between the uncertainties of this particular sub-process. Programming and computational stability limitations in the GMAP program permit estimation of correlations between uncertainties for only a limited number of groups of data sets or data points. Hence, correlations only between uncertainties of different data sets were introduced between strongly correlated data sets. A total of nine groups of correlated data sets were constructed containing {611, 617, 616, 615, 644, 1038, 640, 637}, {608, 609,619,671,672,628}, {660–663, 678, 679, 630, 631}, {1024, 534–536,551}, {676, 677, 680–682, 589}, {547–549 }, {602, 685, 653,654, 605, 666,668}, {407,626,837} and {8002, 1014}.

Table 4: For each ^{239}Pu(n,f) cross-section data set in the GMA database, the GMA number and reference are listed along with its observable ("s" flags shape data). It is also indicated which uncertainty sources, δ, were either added or changed following the literature/ EXFOR or the template. It is also listed whether δo components were added.

GMA #	Observable	Added δ (lit./EXFOR)	Added δ (template)	Changed δ (lit./EXFOR)	Changed δ (template)	δo δo
407 [35]	$\frac{^{239}\mathrm{Pu(n,f)}}{^{238}\mathrm{U(n,\gamma)}}$ s	$\delta\zeta$	$\delta\beta$, $\delta\zeta$, δd	-	$\delta\varepsilon$	N
521 [60]	^{239}Pu(n,f) s	$\delta\zeta$	$\delta\beta$	δ_{ND}	-	Y
534 [61]	$\frac{^{239}\mathrm{Pu(n,f)}}{^{10}\mathrm{B(n,\alpha)}}$ s	$\delta\zeta$	$\delta\zeta$, δd, δm, $\delta\beta$	δb	$\delta\varepsilon$	Y
535 [61]	$\frac{^{239}\mathrm{Pu(n,f)}}{^{6}\mathrm{Li(n,t)}}$ s	$\delta\zeta$, $\delta\varepsilon$	$\delta\zeta$, δd, δm, $\delta\beta$	δb	-	N
536 [62]	$\frac{^{239}\mathrm{Pu(n,f)}}{^{235}\mathrm{U(n,f)}}$ s	-	δm, $\delta\beta$, δd, $\delta\zeta$	-	δb	Y
547 [63]	$\frac{^{239}\mathrm{Pu(n,f)}}{^{6}\mathrm{Li(n,t)}}$ s	$\delta\zeta$	$\delta\zeta$, δd, δm, $\delta\beta$	-	$\delta\varepsilon$	Y
548 [63]	$\frac{^{239}\mathrm{Pu(n,f)}}{^{10}\mathrm{B(n,\alpha)}}$ s	$\delta\zeta$	$\delta\zeta$, δd, δm, $\delta\beta$	-	$\delta\varepsilon$	Y
549 [63]	$\frac{^{239}\mathrm{Pu(n,f)}}{^{235}\mathrm{U(n,f)}}$ s	$\delta\zeta$	$\delta\beta$, δm, δd, $\delta\zeta$	-	-	Y
551 [64]	$\frac{^{239}\mathrm{Pu(n,f)}}{^{10}\mathrm{B(n,\alpha)}}$ s	$\delta\zeta$	$\delta\zeta$, δd, δm, $\delta\beta$		$\delta\varepsilon$	Y
589 [18]	^{239}Pu(n,f) s	δm, $\delta\zeta$	$\delta\beta$, δd, $\delta\zeta$	$\delta\varepsilon$, δb, $\delta\phi$	-	N
600 [65]	$\frac{^{239}\mathrm{Pu(n,f)}}{^{235}\mathrm{U(n,f)}}$	Time shift unc., δd	$\delta\zeta_1$, $\delta\zeta_R$, $\delta\beta$, $\delta\alpha$	δm	$\delta\varepsilon$	Y
602 [28]	$\frac{^{239}\mathrm{Pu(n,f)}}{^{235}\mathrm{U(n,f)}}$	$t_{1/2}^{234}$U, $t_{1/2}^{239}$Pu, $\delta\zeta$	$\delta\beta$, $\delta\alpha$, δb	δN, $\delta\varepsilon$,δd	δN, δm	Y
605 [29]	$\frac{^{239}\mathrm{Pu(n,f)}}{^{235}\mathrm{U(n,f)}}$	-	δm, $\delta\alpha$, $\delta\zeta_R$, $\delta\varepsilon$, $\delta\alpha$	δN_1, δN_R, $\delta\beta$	$\delta\zeta_1$	Y
608 [30]	$\frac{^{239}\mathrm{Pu(n,f)}}{^{235}\mathrm{U(n,f)}}$	Thickness unc.	$\delta\zeta_1$, $\delta\zeta_R$, δd	-	-	Y
609 [31]	$\frac{^{239}\mathrm{Pu(n,f)}}{^{235}\mathrm{U(n,f)}}$	Thickness unc.	$\delta\zeta_1$, $\delta\zeta_R$, δd	-	-	N
611 [32]	^{239}Pu(n,f)	δN, $\delta\alpha$	-	$\delta\varepsilon$, δN, δm, δb	-	N
612 [33]	^{239}Pu(n,f)	-	δd, δm	-	$\delta\phi$, $\delta\varepsilon$	Y
615 [32]	^{239}Pu(n,f)	δE			$\delta\phi$	N
616 [32]	^{239}Pu(n,f)	δE		ε, cone-eff. thickn-unc.		N
617 [32]	^{239}Pu(n,f)	δE		$\delta\beta$, δb, δm	$\delta\phi$	Y
619 [66]	^{239}Pu(n,f)	-	δm, δd, $\delta\zeta$	-	-	N
620 [34]	^{239}Pu(n,f)	-	$\delta\zeta$, δd	-	-	Y
621 [34]	^{239}Pu(n,f)	-	$\delta\zeta$, δd	-	-	N
622 [34]	^{239}Pu(n,f)	-	$\delta\zeta$, δd	-	-	Y
623 [34]	^{239}Pu(n,f)	-	$\delta\zeta$, δd	-	-	Y
626 [35]	$\frac{^{239}\mathrm{Pu(n,f)}}{^{235}\mathrm{U(n,f)}}$ s	-	$\delta\beta$, $\delta\alpha$, $\delta\zeta$	-	-	Y
628 [36]	^{239}Pu(n,f)	-	δd, $\delta\beta$, $\delta\zeta$	δc, $\delta\phi$, δN	-	N
630 [67]	$\frac{^{239}\mathrm{Pu(n,f)}}{^{10}\mathrm{B(n,\alpha)}}$ s	-	$\delta\zeta$, δd	-	$\delta\varepsilon$, δm, $\delta\beta$	N
631 [67]	$\frac{^{239}\mathrm{Pu(n,f)}}{^{235}\mathrm{U(n,f)}}$	-	$\delta\zeta_1$, $\delta\zeta_R$, δd, $\delta\alpha$	-	-	Y
633 [68]	$\frac{^{239}\mathrm{Pu(n,f)}}{^{235}\mathrm{U(n,f)}}$	-	δd	-	-	N
635 [69]	$\frac{^{239}\mathrm{Pu(n,f)}}{^{235}\mathrm{U(n,f)}}$ s	-	δm, δd	$\delta\varepsilon$	$\delta\zeta$	Y
637 [37]	$\frac{^{239}\mathrm{Pu(n,f)}}{^{235}\mathrm{U(n,f)}}$	-	$\delta\varepsilon$, $\delta\zeta$	δc, δm	δN_R	N
640 [38]	^{239}Pu(n,f)	Det. spacing unc.	δd, $\delta\zeta$, δb	-	-	N
644 [27]	^{239}Pu(n,f)	δN, $\delta\alpha$	δE, δd	$\delta\varepsilon$	$\delta\phi$	Y
653 [39]	$\frac{^{239}\mathrm{Pu(n,f)}}{^{235}\mathrm{U(n,f)}}$	$\delta\zeta$, δd	$\delta\beta$, δb	-	δN	Y
654 [39]	$\frac{^{239}\mathrm{Pu(n,f)}}{^{235}\mathrm{U(n,f)}}$ s	δb, $\delta\zeta_1$, $\delta\zeta_R$, δd, $\delta\beta$	-	-		Y
657 [70]	^{239}Pu(n,f)	-	$\delta\beta$, δd, $\delta\zeta$	-	-	N
660 [71]	$\frac{^{239}\mathrm{Pu(n,f)}}{^{10}\mathrm{B(n,\alpha)}}$ s	$\delta\zeta$	δm, $\delta\beta$, δd, $\delta\zeta$	-	$\delta\varepsilon$	N

661 [71]	$\frac{^{239}\mathrm{Pu(n,f)}}{^{10}\mathrm{B(n,\alpha)}}$ s	$\delta\zeta$	δm, $\delta\beta$, δd, $\delta\zeta$	-	$\delta\varepsilon$	Y
662 [71]	$\frac{^{239}\mathrm{Pu(n,f)}}{^{10}\mathrm{B(n,\alpha)}}$ s	$\delta\zeta$	δm, $\delta\beta$, δd, $\delta\zeta$	-	$\delta\varepsilon$	N
663 [71]	$\frac{^{239}\mathrm{Pu(n,f)}}{^{10}\mathrm{B(n,\alpha)}}$ s	$\delta\zeta$	δm, $\delta\beta$, δd, $\delta\zeta$	-	$\delta\varepsilon$	Y
666 [40]	$\frac{^{239}\mathrm{Pu(n,f)}}{^{235}\mathrm{U(n,f)}}$	-	$\delta\beta$, δm, δd	-	-	N
668 [72]	$\frac{^{239}\mathrm{Pu(n,f)}}{^{238}\mathrm{U(n,f)}}$	-	$\delta\beta$, δd, $\delta\zeta$, δE	-	-	N
671 [41]	^{239}Pu(n,f) s	$\delta\zeta$, $\delta\beta$, δd	δd	-	-	Y
672 [41]	^{239}Pu(n,f)	δd, $\delta\zeta$	$\delta\beta$, $\delta\zeta$	δN, $\delta\phi$		N
676 [73]	$\frac{^{239}\mathrm{Pu(n,f)}}{^{10}\mathrm{B(n,\alpha)}}$ s	$\delta\zeta$, δd	$\delta\zeta$	-	-	Y
677 [74]	$\frac{^{239}\mathrm{Pu(n,f)}}{^{10}\mathrm{B(n,\alpha)}}$ s	$\delta\zeta$, δd (676)	$\delta\zeta$	-	-	Y
678 [75]	$\frac{^{239}\mathrm{Pu(n,f)}}{^{10}\mathrm{B(n,\alpha)}}$ s	-	$\delta\zeta$, δd	-	-	Y
679 [76]	$\frac{^{239}\mathrm{Pu(n,f)}}{^{10}\mathrm{B(n,\alpha)}}$ s	-	$\delta\zeta$, δd	-	-	Y
680 [77]	$\frac{^{239}\mathrm{Pu(n,f)}}{^{10}\mathrm{B(n,\alpha)}}$ s	$\delta\zeta$	$\delta\zeta$, δm, $\delta\beta$, δd	-	-	Y
681 [78]	$\frac{^{239}\mathrm{Pu(n,f)}}{^{10}\mathrm{B(n,\alpha)}}$ s	$\delta\zeta$	δm, $\delta\alpha$, $\delta\zeta$, δd	$\delta\varepsilon_R$	-	Y
682 [78]	$\frac{^{239}\mathrm{Pu(n,f)}}{^{10}\mathrm{B(n,\alpha)}}$ s	$\delta\zeta$	δm, $\delta\alpha$, $\delta\zeta$, δd	$\delta\varepsilon_R$	-	Y
685 [42]	$\frac{^{239}\mathrm{Pu(n,f)}}{^{235}\mathrm{U(n,f)}}$	Thickness cor., $\delta\varepsilon$	$\delta\beta$, $\delta\alpha$, δb	-	δN, δm	N
719 [79]	$\frac{^{239}\mathrm{Pu(n,f)}}{^{10}\mathrm{B(n,\alpha)}}$ s	-	$\delta\zeta$, δd	-	$\delta\varepsilon$, δm, $\delta\beta$	Y
837 [80]	$\frac{^{239}\mathrm{Pu(n,f)}}{^{238}\mathrm{U(n,f)}}$ s	$\delta\zeta$	$\delta\beta$, δd, $\delta\zeta$	-	-	N
1012 [81]	$\frac{^{239}\mathrm{Pu(n,f)}}{^{235}\mathrm{U(n,f)}}$	-	δm	-	δN	Y
1014 [25]	$\frac{^{239}\mathrm{Pu(n,f)}}{^{235}\mathrm{U(n,f)}}$	-	δm, $\delta\varepsilon$, $\delta\alpha$	δb, $\delta\beta$, $\delta\phi$, δd, $\delta\zeta_1$, $\delta\zeta_R$	δN	Y
1024 [82]	$\frac{^{239}\mathrm{Pu(n,f)}}{^{10}\mathrm{B(n,\alpha)}}$ s	δE, $\delta\varepsilon_1$, $\delta\varepsilon_R$, δb	$\delta\beta$, δm, δd		$\delta\varepsilon_1$	Y
1029 [23]	$\frac{^{239}\mathrm{Pu(n,f)}}{^{235}\mathrm{U(n,f)}}$	$\delta\zeta$, δb	$\delta\varepsilon$, δd, $\delta\zeta$, δm, $\delta\beta$		δN_1, δ_R	Y
1038 [43]	^{239}Pu(n,f)	$\delta\varepsilon$, $\delta\zeta$, $\delta\phi$,δm, $\delta\beta$, δb	δE, δb	δN	-	Y
8002 [24]	$\frac{^{239}\mathrm{Pu(n,f)}}{^{235}\mathrm{U(n,f)}}$ s	-	$\delta\varepsilon$,δd, $\delta\alpha$, $\delta\beta$, δm	-	-	Y

Table 5: Additional comments regarding changes in uncertainties are supplied for particular data sets.

GMA #	Comments
605	Normalization uncertainty split into ^{235}U and ^{239}Pu normalization uncertainties
612	δc and δb are given separately to obtain more realistic correlations
644	δE taken from 611 (same method and E)
1012	Energy resolution uncertainties moved to appropriate entry
1014	Total uncertainties split into partial components following EXFOR
1024	Systematic uncertainty components split according to literature
1029	Sample mass uncertainties were increased to values given by Staples for the same samples, background uncertainty added from [23]
1038	Total systematic uncertainties split into partial components following EXFOR
8002	Data changed to ratio shape data (normalized to thermal point)

Table 6: The values used to estimate correlation coefficients between partial uncertainties of different measurements are listed. This table was applied as follows: If two data sets used, *e.g.*, the same technique to determine the background and δb, the value given in this table for their common technique was used for correlating δb between these two data sets.

Unc. source	Cor. estimate
$\delta N_{(a/b\&c)}$	Same sample and method: 1.0 Relative to therm: 0.8 α-counting: 0.4 (0.3 with different 2^{nd} method)
δc	0
$\delta\beta$ & δm	Monte Carlo simulation: 0.5 for similar materials (0.3 different material) Measured: 0.3
$\delta\varepsilon$ & $\delta\alpha$	Stopping power calculated: 0.8 α-counting for/ measuring roughness: 0.4 Measured forward-boost: 0.5 Calculated forward-boost: 0.8 Monte Carlo simulated geometry: 0.5 Calculated fission-fragment angular distribution: 0.5 Extrapolation: 0.5 Pulse-height-discrimination: 0.1
δb	Meas.: 0 (same facility: 0.5) Monte Carlo simulation: 0.5 Monochromatic/ black resonance filter techniques : 0.2 Pulse-height-discrimination: 0.1
δE	0 (not considered in GMAP analysis)
$\delta\phi$	Associated particle: 0.5 if same reaction Mn bath: 0.5 Recoil proton measurement: 0.5
$\delta\zeta$	α-counting: 0.4 Uncertainty & technique not given: 0.5
δd	0

It is evident from Table 7 that revising the experimental covariances following this procedure leads to distinctly different total uncertainties of individual data sets compared to their original values used in [1]. In many cases the experimental uncertainties are increased. Even more importantly: If one orders the data sets according to the size of their lowest uncertainties, their sequence alters with improving the covariances. This implies that the overall importance of particular data sets in the database, and thus their impact on the evaluation, evolves with modifying uncertainties. Hence, changes in the evaluated cross section and uncertainties can be expected due to the update of these uncertainties.

Table 7: The total experimental uncertainties entering the recent NDS evaluation (Orig. unc.) are compared to updated ones of this work (Updated unc.). The total uncertainties are shown as used for the generalized least-square procedure in GMAP, that is after interpolating the data to a union grid. The GMA numbers of data sets where either the minimum or maximum uncertainties increased are highlighted in bold in the first column. This indicates that the total uncertainties were increased for many data sets in the NDS database. The revised ordering of the data with respect to the smallest uncertainty (Upd. importance) highlights that the weight of individual data sets on the evaluation was modified by revising covariances. Thus, a change in the evaluated cross sections is expected.

GMA #	Orig. unc.	Updated unc.	Upd. importance
407 [35]	3.7–6.3	3.8–6.3	47 → 46
521 [60]	2.3–4.8	3.1–4.2	26 → 33
534 [61]	0.8–3.4	1.9–4.6	5 → 13
535 [61]	2.3–4.1	3.3–5.5	25 → 37
536 [62]	0.6–6.5	0.8–7.7	1 → 2
547 [63]	1.5–5.1	1.6–5.4	13 → 6
548 [63]	1.7–9.6	1.7–11.7	16 → 12
549 [63]	2.0–3.6	1.6–14.8	17 → 7
551 [64]	1.5–7.3	2.0–2.8	12 → 16
589 [18]	2.9–3.9	3.7–4.5	36 → 42
600 [65]	1.7–27.4	1.9–19.6	14 → 14
602 [28]	0.8–6.8	1.5–6.5	3 → 5
605 [29]	1.7–15.3	1.9–16.1	15 → 15
608 [30]	2.0–12.6	2.3–13.6	20 → 23
609 [31]	2.0–2.1	2.3	19 → 20
611 [32]	1.0	1.7	7 → 9
612 [33]	3.8–5.7	3.3–4.2	48 → 38
615 [32]	2.1	2.2	23 → 19
616 [32]	5.4	3.8	53 → 43
617 [32]	5.8	4.2	56 → 49
619 [66]	2.9	3.3	35 → 39
620 [34]	2.8–6.6	2.9–5.9	34 → 29
621 [34]	2.9–3.2	3.0–3.3	37 → 30
622 [34]	2.8–7.0	2.9–7.5	33 → 28
623 [34]	3.2–4.1	3.5–4.4	40 → 41
626 [35]	2.5–3.3	2.6–4.3	31 → 26
628 [36]	5.9	4.4	57 → 50
630 [67]	2.3–5.0	3.0	27 → 31
631 [67]	2.1	2.1–5.2	22 → 18
633 [68]	3.3	3.3	41 → 36
635 [69]	3.1–123.1	3.3–109.2	39 → 35
637 [37]	2.3	2.5	29 → 25
640 [38]	2.4–3.1	2.4–3.1	30 → 24
644 [27]	2.0	5.8	18 → 58
653 [39]	1.2–6.9	1.7–6.2	10 → 11
654 [39]	1.0–5.7	1.0–3.9	8 → 3
657 [70]	9.3	4.4	60 → 51
660 [71]	7.1–7.5	7.2–7.6	59 → 60
661 [71]	6.4–7.7	6.5–8.8	58 → 59

662 [71]	5.4–11.9	5.5–6.1	54 → 55
663 [71]	5.4–15.6	5.5–13.4	52 → 54
666 [40]	5.7–6.2	5.7–6.2	55 → 57
668 [72]	10.3	10.3	61 → 61
671 [41]	4.3–25.8	5.6–27.0	49 → 56
672 [41]	4.9–5.4	5.3–5.7	51 → 53
676 [73]	3.4–32.6	3.4–22.6	42 → 40
677 [74]	3.0–5.7	3.1–5.7	38 → 32
678 [75]	4.7–31.6	4.7–29.2	50 → 52
679 [76]	3.7–20.1	3.8–16.5	46 → 45
680 [77]	3.7–4.2	3.8–6.0	43 → 44
681 [78]	3.7–8.2	4.0–8.9	45 → 47
682 [78]	3.7–10.0	4.0–10.6	44 → 48
685 [42]	1.1	2.0	9 → 17
719 [79]	2.2–15.6	3.1–17.0	24 → 34
837 [80]	2.6–3.7	2.7–3.7	32 → 27
1012 [81]	2.1–5.8	2.3–6.6	21 → 21
1014 [25]	1.3–1.6	1.7–3.9	11 → 10
1024 [82]	0.8–4.6	1.6–3.1	4 → 8
1029 [23]	1.0–2.5	1.5–2.8	6 → 4
1038 [43]	2.3–7.7	2.3–6.8	28 → 22
8002 [24]	0.7–3.8	0.8–4.4	2 → 1

4 RESULTS AND DISCUSSION

4.1 Impact of Improved ^{239}Pu(n,f) Experimental Covariances on Evaluated Results

The impact of revising the ^{239}Pu(n,f) experimental covariances in the GMA database on the evaluated cross sections and uncertainties is studied here for various observables in GMA. To this end, the full GMA database—including the updates in the ^{239}Pu(n,f) experimental covariances—was used for a GMAP fit across many observables, similarly to the evaluation for [1]. It should be emphasized that only the ^{239}Pu(n,f) experimental covariances were modified while the data and covariances of all other data sets were carried over unchanged—including their δo values assigned for the evaluation in Ref. [1]. Also, the experimental mean values of all ^{239}Pu(n,f) cross sections remained the same.

If missing uncertainties of single experimental data sets are added into the GMA database, and underestimated ones are modified for individual data sets based on literature and the template (steps 1–3 in Section 3), the evaluated mean values and standard deviations change distinctly as can be seen in Fig. 1. The mean values differ by up to 3% at a few specific E, with a mean difference in the cross section across all E of a non-negligible 0.4%. The uncertainties increase at many E leading to a mean increase of 2.1% across all E. However, from 2 keV to 300 keV, they decrease significantly. This decrease might at first seem counter-intuitive given that additional uncertainties were included in most cases and increased in others. However, the original δo had to be removed as described in Section 3. When δo is re-determined and then re-introduced, the resulting mean values change less drastically compared to [1] and the associated standard deviations increase, as expected, at most E. The maximum difference in the cross section now does not exceed values of 2% with a mean change across all energies of 0.09% that is smaller than before adding δo. The evaluated uncertainties increase at most E except for 10–200 keV. In this energy range, δt_e of single experiments was sufficiently large that the δo was zero contrary to [1] where δo was included leading to overall larger uncertainties for these particular data sets. Considering correlations between uncertainties of different experiments leads to only a small difference in the evaluated cross section compared to including δo. The mean change of the cross section is now decreased to 0.07% as can be seen in Table 8, with deviations from [1] as large as ±2% at specific energies. Differences of about 2% can be observed, for instance, close to 14 MeV. At this energy, there are some data sets (611, 644, 685, 8002, 609) which originally had low uncertainties but, on revision, had substantial uncertainties introduced, thereby contributing to the significant differences observed in the cross section. The cross section also deviates significantly at 200–600 keV from [1]. In this energy range, $\delta\beta$ is non-negligible, but it was missing for many data sets. Consistently considering $\delta\beta$ likely contributed non-negligibly to the changes in that particular energy range. The evaluated uncertainties differ distinctly—especially up to 10 keV. In this particular energy range, earlier many physically justifiable correlations were missing between uncertainties of different data sets, while non-zero correlations between uncertainties of data sets influencing the evaluated data above 10 keV were already present in the original

GMA database. Below 10 keV, many ^{239}Pu(n,f) GMA data sets were measured relative to ^{10}B(n,α) and two relative to ^{6}Li(n,α). Seven out of these 20 data sets were undertaken by the group of Gwin/Weston (1024, 534, 677, 676, 681, 682, 535), three by the Wagemans group (547–549 with 549 relative to ^{235}U) and four by Ryabov (660–663). The correlations between uncertainties of these data sets within a group were only scarcely quantified, and in many cases they were entirely neglected. Therefore, a bigger change of evaluated uncertainties is observed in the energy range below 10 keV than elsewhere.

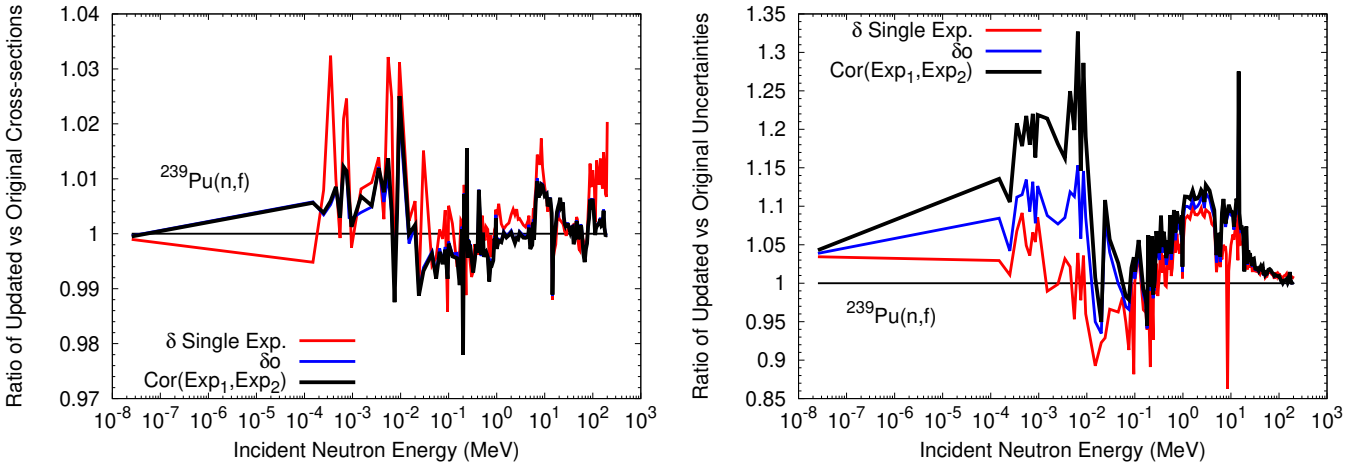

Figure 1: (Color Online) Evaluated mean values (left-hand side) and uncertainties (right-hand side) of ^{239}Pu(n,f) cross sections are shown as ratios to the evaluated mean values and uncertainties obtained from GMAP for the recent NDS Evaluation [1]. One evaluation was obtained after updating the GMA database according to steps 1–3 in Section 3 (adding missing uncertainties of single experiments), steps 1–4 (additionally adding δo) and steps 1–5 (additionally adding correlations between uncertainties of different experiments). Note that USU are not included in any of these plots.

Table 8: The differences in evaluated cross section (cs) and uncertainties (unc.) observed between the recent NDS evaluation and GMAP code results obtained after updating ^{239}Pu(n,f) covariances in the GMA database are tabulated for various reaction cross sections.

Reaction	Range of		Mean change of	
	cs change	unc. change	cs	unc.
^{6}Li(n,α)	1.0–1.002	0.999–1.035	1.0	1.002
^{10}B(n,α_0)	1.0	1.0	1.0	1.0
^{10}B(n,α_1)	1.0	0.998–1.001	0.9999	1.0
Au(n,γ)	0.998–1.001	0.998–1.001	0.9994	1.0
^{235}U(n,f)	0.994–1.002	0.978–1.063	0.9988	1.006
^{238}U(n,γ)	0.998–1.001	0.999–1.005	0.9996	1.001
^{239}Pu(n,f)	0.978–1.025	0.944–1.327	1.0007	1.062

In general, it is obvious that including missing uncertainties of single data sets by referring to the template and retrieving detailed information from literature leads to an overall increase of evaluated uncertainties. However, even more importantly, evaluated mean values change in a non-negligible manner. This difference in the cross section was expected since the increased experimental uncertainties of specific data sets change their impact on the evaluation relative to other data sets in the database. Some data sets (*e.g.*, 611, 534, 685) which previously had a high impact, now have a lower impact, and this leads to an altered cross section. In contrast, the cross section did not change when USU were added *a-posteriori* to the most recent NDS evaluated uncertainties originally obtained from the GMAP code. It was already shown in Ref. [8] that the evaluated mean values are expected to change if the USU are added *a-priori*, that is to the experimental covariances in the GMA database.

Hence, the first conclusion of this paper is that indeed **uncertainties of single experimental data sets and correlations between them were missing for many** ^{239}Pu(n,f) cross-section **data sets in the GMA database**. It is very likely that this is true for data sets of other observables in the GMA database given that some of the ^{239}Pu(n,f) cross-section data sets were measured as part of a series that provided GMA data sets for other observables. Hence,

an increase of the evaluated uncertainties by expert judgment was justified. However, the approach taken earlier to enhance these uncertainties is shown in this paper to be oversimplified. Furthermore, then overlooked details, when properly considered, are presumably leading to more correct evaluated mean values than were produced in earlier evaluations neglecting this information.

However, one might argue that the evaluated uncertainties increased by USU are still distinctly larger than those uncertainties obtained by updating the uncertainty and correlation information for ^{239}Pu(n,f) cross-section data sets, as can be seen in Fig. 2. Hence, one could question whether the ^{239}Pu(n,f) cross-section uncertainties in ENDF/B-VIII.0 are over-estimated. One part of this discrepancy could be attributed to the fact that not all physically justifiable correlations between uncertainties of different experiments can be accounted for. This effect is, however, unlikely to lead to a significantly increased standard deviation since the groups of correlated data were chosen such that data outside of these groups had smaller correlations.

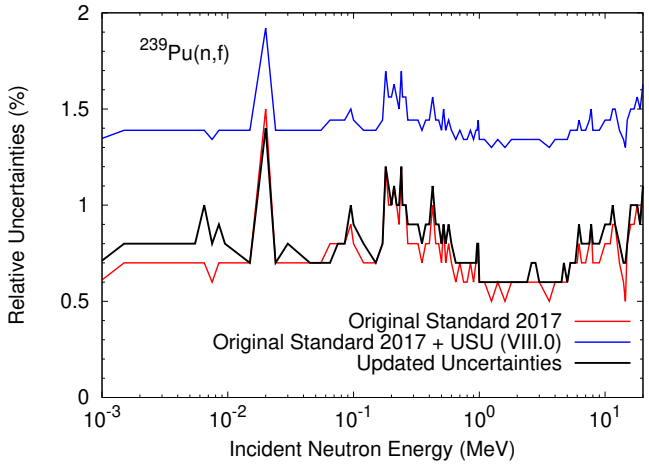

Figure 2: (Color Online) The final evaluated uncertainties of ^{239}Pu(n,f) cross sections of this work are compared to those originally obtained from the code GMAP for [1] and those enlarged by USU. The latter uncertainties were included in the ENDF/B-VIII.0 database.

A larger increase of evaluated uncertainties is to be expected from revising covariances of all data sets in the GMA database, especially those for which ^{239}Pu(n,f) cross sections are measured as ratios to. Some of the ^{239}Pu(n,f) cross sections are measured relative to ^{235,238}U(n,f), ^{238}U(n,γ), ^{10}B(n,α) and ^{6}Li(n,α). The evaluated mean values and uncertainties of some of these observables now differ from the values of [1] just by updating the ^{239}Pu(n,f) covariances. For instance, the ^{235}U(n,f) cross section and its uncertainties change non-negligibly in Fig. 3. Of course, these deviations from [1] are less pronounced than for the ^{239}Pu(n,f) cross section, but they mirror its behavior, especially, in those energy regions with many ^{239}Pu(n,f) cross-section data sets in GMA that involve ^{235}U(n,f) (above 100 keV). It is noteworthy that the ^{10}B(n,α_0) and ^{10}B(n,α_1) cross sections and uncertainties remain nearly the same despite the fact that uncertainties of the ^{239}Pu(n,f)/^{10}B(n,α) data in some cases change significantly as can be seen from Tables 4 and 7. One explanation for this could be that the ^{10}B(n,α_0) and ^{10}B(n,α_1) cross sections are mostly defined by the R-matrix calculated data sets explicitly considered in the GMA database. Some of these data were calculated by the Los Alamos National Laboratory R-matrix analysis code EDA [85]. These data have rather low uncertainties in the range of 0.2–1.4% for these EDA data of ^{10}B(n,α_1) and 0.2–2.1% for EDA data of ^{10}B(n,α_0) and, hence, dominate the evaluation compared to the impact of data sets as ratios to these observables which have often higher uncertainties.

It is equally noteworthy, however, that small differences in the Au(n,γ) cross section and its uncertainties are observed in Fig. 4 by revising ^{239}Pu(n,f) covariances in GMA. There is not a single data set in the whole GMA database for ^{239}Pu(n,f) as a ratio to the Au(n,γ) reaction. This example illustrates that many, if not all, observables in the GMA database are impacted—at least to a certain level—by improving covariances of experimental data of a single observable due to cross-correlations and ratio data sets across all observables in the database.

This leads to the second conclusion that the **covariances of all observables in the database need to be improved in order to arrive at fully re-quantified cross sections and uncertainties of the ^{239}Pu(n,f) reaction along with all other NDS project evaluated observables within the GMA database.** To this end, templates of expected uncertainties for other observables, *e.g.*, (n,γ) or (n,α) measurements are needed to aid in a comprehensive uncertainty analysis across many data sets. The template presented here can be used to update uncertainties of ^{235,238}U(n,f) cross-section data sets in the GMA database.

It should also be highlighted that applying the template of expected uncertainties presented here to updating

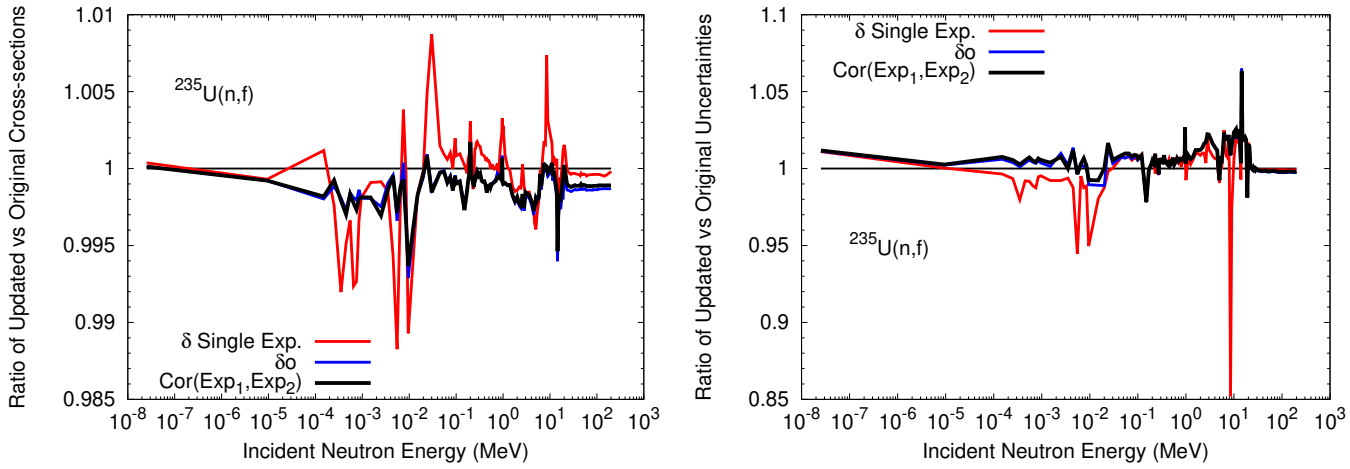

Figure 3: (Color Online) The same as Fig. 1 is shown for the ^{235}U(n,f) cross section and its associated uncertainties.

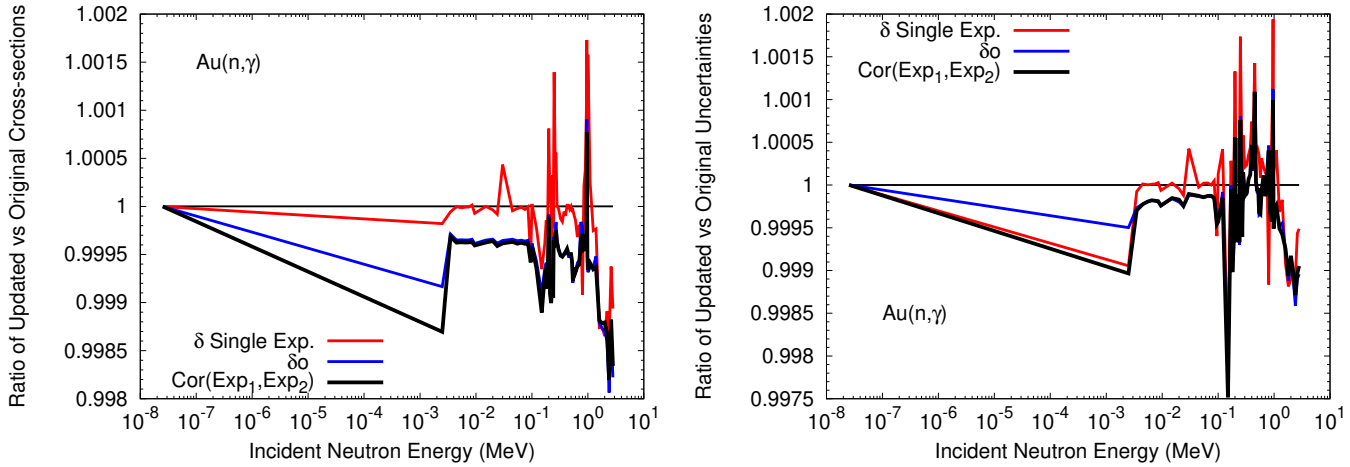

Figure 4: (Color Online) The cross section and associated uncertainties are shown for Au(n,γ) in the same manner as in Fig. 1.

covariances only accounts for *known* uncertainty sources. Even after improving covariances of all data sets in the GMA database using templates, one might then observe a larger scatter in the data than expected from the evaluated uncertainties. This larger scatter might be caused by underlying unknown biases and statistical perturbations in the data that influence the evaluations. Hence, unknown uncertainties applying to many data sets using, *e.g.*, a specific technique that could have unknown flaws, might be missing. They can be quantified following procedures outlined in Ref. [4]. These unknown uncertainties might perhaps become knowable by undertaking measurements of the same observables, for which a large scatter is observed, with different techniques. For instance, one example would be employing a time projection chamber for measuring fission fragments instead of a fission chamber [14, 16, 15]. This notion is summarized in the third conclusion: Templates of expected uncertainties only allow the addition of missing covariances for known uncertainty sources. **USU cannot be addressed by the template, and can be either reduced or eliminated by using novel measurement techniques to explore these unknown effects in a targeted manner or they need to be quantified separately.** Hence, the hope is that by using templates, it is possible to decrease the need for a USU treatment following Ref. [4] but may not eliminate it altogether.

4.2 Impact of Modified Evaluated ^{239}Pu(n,f) Cross Sections on Benchmark Simulations

The revised ^{239}Pu(n,f) cross sections were used to simulate a small set of ICSBEP critical assemblies [86, 87] and one plutonium LLNL pulsed sphere [88, 90, 89]. This study enables assessment of whether the changes highlighted in Fig. 1 impact benchmarks representative of application calculations in a non-negligible way. To this end, all benchmarks calculations were performed once with MCNP-6.1.1 [91] using ENDF/B-VIII.0. The resulting benchmark values are

compared in Table 9 and Fig. 5 to experimental data as well as to values calculated with ENDF/B-VIII.0 [92] for all data excluding ^{239}Pu(n,f) cross sections from 95 keV to 20 MeV. In this energy range, the cross sections of this work were used. This new file was produced with DECE [93] and NJOY-2016 [94]. Data below 95 keV were not used from this new evaluation since unresolved resonance structures in the cross sections are already visible that change rapidly with smaller changes in the GMA database.

The average neutron multiplication factors, $k_{\rm eff}$, of the selected plutonium metal fast (PMF) assemblies decrease by 72–109 pcm with the new ^{239}Pu(n,f) evaluated cross section. This difference is significant as it is close to or more than one third of a dollar for a plutonium system, the change between a controlled and uncontrolled system. Only one plutonium solution thermal (PST) assembly was calculated which differs only within the Monte Carlo statistical uncertainties. This was expected since the $k_{\rm eff}$ sensitivities with respect to the ^{239}Pu(n,f) cross section are a factor of 20 smaller than those of the PMF benchmarks for neutrons in the energy range 95 keV–20 MeV. The PMI ("I" for intermediate spectrum) $k_{\rm eff}$ change amounts to a non-negligible 77 pcm. While its $k_{\rm eff}$ is at 1 MeV by approximately a factor of three less sensitive to the ^{239}Pu(n,f) cross section, it is similarly sensitive to the cross section for E =100–300 keV where non-negligible modification are observed in Fig. 1.

Table 9: The difference in C/E values $k_{\rm eff}$, $\Delta k_{\rm eff} = k_{\rm eff}^{\rm upd.} - k_{\rm eff}^{\rm VIII.0}$, is shown for the two cases where either a modified version of ENDF/B-VIII.0, that includes the resulting ^{239}Pu(n,f) cross section of this work from 950 keV to 20 MeV, or just the unmodified version of ENDF/B-VIII.0 is employed for simulating various critical assemblies. The simulated $k_{\rm eff}$ uncertainties are tabulated in brackets in pcm.

Benchmark	C/E $k_{\rm eff}$ VIII.0	C/E $k_{\rm eff}$ upd. ^{239}Pu(n,f) cs	Δ $k_{\rm eff}$ (pcm)
PMF001	0.99981 (8)	0.99892 (8)	-89
PMF002	1.00147 (8)	1.00075 (8)	-72
PMF006	0.99978 (10)	0.99869 (10)	-109
PMI002	1.00393 (7)	1.00316 (7)	-77
PST034.10	0.99652 (16)	0.99653(22)	1

The LLNL pulsed sphere TOF spectrum, in Fig. 5, calculated with the new cross section changes in a statistically significant way from the ENDF/B-VIII.0 calculated values only in the TOF flight range right after the peak and in the valley. Recent work of Ref. [95] has explored the sensitivities of the neutron leakage spectrum of a ^{235}U LLNL pulsed sphere with respect to several nuclear data observables. This work indicates that the calculated LLNL pulsed sphere neutron-leakage spectrum has non-negligible sensitivities to the (n,f) cross section from 13–15 MeV in the TOF range right after the peak and in the valley, but is only negligibly sensitive to (n,f) cross sections at other energies. Changes in the neutron-leakage spectrum calculated with ENDF/B-VIII.0 versus ENDF/B-VIII.0 modified with the ^{239}Pu(n,f) cross section presented here that extend from -1.2% to 0.6% are visible in this particular TOF range. It can be assumed that this difference is caused by the changes in the ^{239}Pu(n,f) cross section close to 14 MeV.

The results discussed above lead to the fourth conclusion: **The evaluated cross section and its uncertainties change distinctly when the experimental ^{239}Pu(n,f) covariances in the GMA database are improved using literature and the template. This difference in the evaluated cross section has a significant impact on the criticality of selected benchmarks simulated with these data.** It should be re-iterated that the complete GMA database needs to be updated to fully re-assess any observable evaluated with the NDS code and database.

5 SUMMARY, CONCLUSIONS AND OUTLOOK

The uncertainties of individual experiments, and correlations between them, were revised for all ^{239}Pu(n,f) cross-section experiments in the Neutron Data Standards (NDS) database, GMA, using the respective literature and a template of uncertainties expected to appear in (n,f) measurements. This particular cross section and evaluation was chosen as it was suspected that uncertainties of single experiments, correlations between those of different experiments, and unknown systematic uncertainties across many data sets were missing in the database. As the evaluation is mainly based on experimental data, this missing uncertainty information was expected to have a significant impact on both evaluated mean values and covariances. Hence, the evaluated uncertainties of, *e.g.*, the ^{239}Pu(n,f) cross section were increased *a-posteriori* for ENDF/B-VIII.0 by USU (unrecognized sources of uncertainties) to account broadly for this effect. A template of expected uncertainties in (n,f) measurements was used to consistently and systematically identify missing or underestimated uncertainties of single experiments and to add missing correlations, thereby limiting the

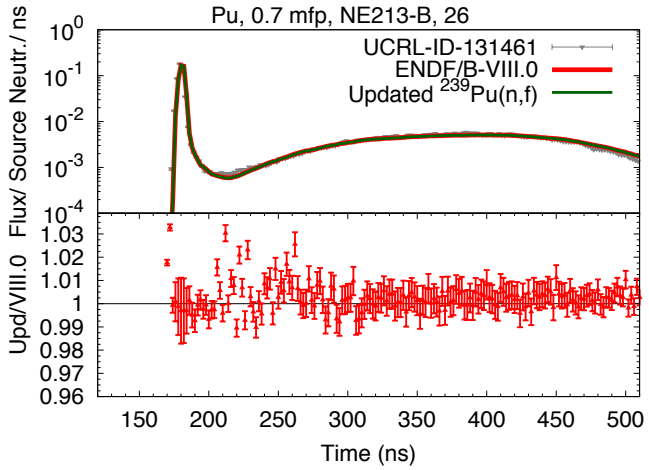

Figure 5: (Color Online) The simulated and experimental neutron-leakage TOF spectra of a plutonium LLNL pulsed sphere are compared in the upper panel of the plot. In one case, it is calculated with ENDF/B-VIII.0 including the resulting ^{239}Pu(n,f) cross section of this work from 950 keV to 20 MeV, and in the other case only with ENDF/B-VIII.0. The lower panel of this plot shows the ratios derived from these two sets of calculations.

need for USU. The updates to the original template of Ref. [9] are highlighted in Section 2.

The main conclusions from this work to improve the ^{239}Pu(n,f) covariances in the GMA database are:

- Uncertainties of single experimental data sets and correlations between those of different experiments were indeed missing for ^{239}Pu(n,f) cross-section data in GMA. It is likely that the same is true for experimental data of other data sets in GMA.
- Including this missing information, with reference to the literature of the experiments and the template, led to an overall increase in evaluated uncertainties. Even more important, the cross sections were sufficiently changed to significantly impact the calculated average neutron multiplication factor, k_{eff}, of selected plutonium critical assemblies. Changes of approximately 72–109 pcm, that is about a third of the difference between a controlled and an uncontrolled plutonium system, were observed for a few fast assemblies.
- The revised ^{239}Pu(n,f) covariances in the GMA database impacted other observables through cross-correlations between measurement uncertainties of different observables and ratio measurements. Hence, an update of covariances of all observables in GMA is needed for a comprehensive, simultaneous re-assessment of mean values and uncertainties of all observables.
- The updated evaluated standard deviations of the ^{239}Pu(n,f) cross section are lower than those of ENDF/B-VIII.0 which were enlarged *a-posteriori* by inclusion of an USU component after carrying out a least-squares evaluation process using the code GMAP. One reason that this might have been the case could be missing uncertainties of other data sets. However, some unrecognized sources of uncertainties across many measurements performed using the same (flawed) technique, or for some other unknown reasons, might still be missing. Therefore, a thorough investigation to determine whether this is the case needs to be carried out after a GMAP evaluation is performed using comprehensive and realistic uncertainties and correlations for all known uncertainty sources, and encompassing all observables in the GMA dataset. Templates of uncertainties only address known missing uncertainties and can thus only reduce the need for USU but may not fully eliminate it. The need to resort to inclusion of USU components can be avoided only by resorting to detailed as well as novel measurement and data analysis techniques that offer the possibility of uncovering true sources of uncertainties that hitherto were unknown to experimenters and, if possible, eliminating the need for USU by applying corrections to the measured data.

In summary, a template of expected uncertainties provides a viable tool for nuclear data evaluators to identify possible missing uncertainties and correlations that have the potential to impact benchmark calculations that are representative of important application calculations.

In order to update the full GMA database and for nuclear data evaluations in general, more templates for uncertainties of different observables (*e.g.*, neutron-induced charged particle reactions, prompt fission neutron spectra, (n,γ) reactions) are needed. There is currently an initiative ongoing within the CSEWG community to create more of these templates for use by evaluators, experimentalists, EXFOR compilers and journal editors.

Acknowledgments D.N. thankfully acknowledges collaborations with B.E. Hejnal and D.E. Vaughan for beginning work on the fission cross-section uncertainty template documented in Ref. [9]. The advice of T. Kawano and W. Haeck in generating ENDF-6 and ACE formatted files of the neutron-induced fission cross section is also gratefully acknowledged. D.N. also thanks P. Obložinský for his detailed feedback on the manuscript. Last but not least, the lead author would like to thank D.L. Smith for his extensive and invaluable help in editing the language of the manuscript. (LA-UR-19-23127) Work at Los Alamos National Laboratory was carried out under the auspices of the NNSA of the U.S. Department of Energy under Contract 89233218CNA000001. (LLNL-JRNL-783165) Work at Lawrence Livermore National Laboratory was performed under the auspices of the U.S. Department of Energy by Lawrence Livermore National Laboratory under Contract DE-AC52-07NA27344.

References

[1] A.D. Carlson, V.G. Pronyaev, R. Capote *et al.*, "Evaluation of the Neutron Data Standards," Nucl. Data Sheets **148**, 143–188 (2018).

[2] A.D. Carlson, V.G. Pronyaev, D.L. Smith *et al.*, "International Evaluation of Neutron Cross Section Standards," Nucl. Data Sheets **110**, 3215–3324 (2009).

[3] E.V. Gai, "On the Problem of Ambiguity of the Evaluated Nuclear Data Uncertainties," International Atomic Energy Agency Report INDC(NDS) 0750 (2018).

[4] R. Capote, S. Badikov, A.D. Carlson *et al.*, "Unrecognized Sources of Uncertainties (USU) in Experimental Nuclear Data," Nucl. Data Sheets, in preparation (2020).

[5] W.P. Poenitz and S.E. Aumeier, "The Simultaneous Evaluation of the Standards and Other Cross-Sections of Importance for Technology,"Argonne National Laboratory Report ANL/NDM-139 (1997).

[6] S.A. Badikov, Z. Chen, A.D. Carlson *et al.*, "International Evaluation of Neutron Cross-section Standards,"International Atomic Energy Agency Report STI/PUB/1291 (2007).

[7] GMAP is the original GMA code [5] extended with the Chiba-Smith algorithm to address Peelle's Pertinent Puzzle [6, 2] by V. Pronyaev. GMA was named after Gauss, Markov and Aitken.

[8] R. Capote and D. Neudecker, "How Accurately we Know the standard ^{252}Cf(sf) Neutron Multiplicity?," Proceedings of the Advances in Nuclear Nonproliferation Technology and Policy Conference 2018 Orlando, FL, November 11–15, 2018 (2019).

[9] D. Neudecker, B. Hejnal, F. Tovesson *et al.*, "Template for Estimating Uncertainties of Measured Neutron-induced Fission Cross-sections," Europ. Phys. J. N **4**, 21 (2018).

[10] P. Schillebeeckx, B. Becker, Y. Danon *et al.*, "Determination of Resonance Parameters and their Covariances from Neutron Induced Reaction Cross Section Data,"Nucl. Data Sheets 113, 3054–3100 (2012).

[11] P. Helgesson, H. Sjöstrand and D. Rochman, "Uncertainty-driven Nuclear Data Evaluation Including Thermal (n,α) Applied to ^{59}Ni," Nuclear Data Sheets, **145**, 1–24 (2017).

[12] A.M. Lewis, "Experimental and Modeling Uncertainties in Cross Section Measurements Utilizing Partial Gammas,"Los Alamos National Laboratory Report LA-UR-18-26628 (2018), publication in preparation.

[13] N.S. Bowden, M. Heffner, G. Carosi *et al.*, "Directional Fast Neutron Detection Using a Time Projection Chamber," Nucl. Instrum. Methods Phys. Res. Sect A **624**, 153–161 (2010).

[14] M. Heffner, D.M. Asner, R.G. Baker *et al.*, "A Time Projection Chamber for High Accuracy and Precision Fission Cross-section Measurements," Nucl. Instrum. Methods Phys. Res. Sect A **759**, 50–64 (2014).

[15] L. Snyder, B. Manning, N.S. Bowden *et al.*, "Performance of A MICROMEGAS-based FissionTPC in a High-energy Neutron Beam," Nucl. Instrum. Methods Phys. Res. Sect A **881**, 1 (2018).

[16] R.J. Casperson, D.M. Asner, J. Baker *et al.*, "Measurement of the Normalized ^{238}U(n,f)/^{235}U(n,f) Cross Section Ratio from Threshold to 30 MeV with the NIFFTE fission Time Projection Chamber," Phys. Rev. C **97**, 034618 (2018).

[17] A.D. Carlson, W.P. Poenitz, G.M. Hale *et al.*, "ENDF/B-VI Neutron Cross Section Measurement Standard," Brookhaven National Laboratory Report ENDF-351 (1993).

[18] D.B. Gayther, D.A. Boyce and J.B. Brisland, "Measurement of the ^{235}U Fission Cross-Section in the Energy Range 1 keV to 1 MeV,"Panel on Neutron Standard Reference Data, Vienna 1972, 201-211 (1972); D.B. Gayther, "Measurement of the ^{239}Pu Fission Cross-section and its Ratio to the ^{235}U Fission Cross-section in the Energy Range from 1 keV to 1 MeV,"Proc. of the Conf. on Nucl. Cross-sections and Technol., Washington 1975, **2**, 564–567 (1975).

[19] H.G. Hicks, H.B. Levy, W.E. Nerkiv *et al.*, "Further Radiochemical Studies of Fission of the U^{236*} Compound Nucleus,"Phys. Rev. **128**, 700–707 (1962).

[20] In GMA, a linearly decreasing correlation matrix with respect to the difference in energy between two data points is usually preferred to avoid strongly correlated covariances which increase the χ^2 value.

[21] In some measurements, the uncertainty arising from correcting the sample mass due to illuminating only part of the sample is termed "geometry" uncertainty.

[22] C. Jammes, P. Filliatre, P. Loiseau *et al.*, "On the Impact of the Fissile Coating on the Fission Chamber Signal,"Nuclear Inst. and Methods in Phys. Res. A **681**, 101–109 (2012).

[23] P.W. Lisowksi, J.L. Ullmann, S.J. Balestrini *et al.*, "Neutron Induced Fission Cross Section Ratios for ^{232}Th, ^{235,238}U, ^{237}Np and ^{239}Pu from 1 to 400 MeV,"Proc. of the Conf. on Nucl, Data for Science and Technol., Mito 1988, 97–99 (1988); P.W. Lisowksi, A. Gavron, W.E. Parker *et al.*, "Fission Cross Sections in the Intermediate Energy Region,"Proc. of a Specialists' Meeting on Neutron Cross Section Standards for the Energy Region above 20 MeV, Report NEANDC-305, 177–186 (1991); A.D. Carlson, O.A. Wasson, P.W. Lisowski *et al.*, "A Study of the ^{235}U(n,f) Cross Section in the 3 to 30 MeV Energy Region,"Proc. of the Conf. on Nucl, Data for Science and Technol., Mito 1988, 1029–1032 (1988).

[24] F. Tovesson and T.S. Hill, "Cross Sections for ^{239}Pu(n,f) and ^{241}Pu(n,f) in the Range E_n = 0.01 eV to 200 MeV,"Nucl. Science and Eng. **165**, 224–231 (2010) (Pu-9); F. Tovesson and T.S. Hill, "Subthreshold Fission Cross Section of ^{237}Np,"Nucl. Science and Eng. **159**, 94–101 (2008).

[25] P. Staples and K. Morley, "Neutron-Induced Fission Cross-Section Ratios for ^{239}Pu, ^{240}Pu, ^{242}Pu, and ^{244}Pu Relative to ^{235}U from 0.5 to 400 MeV,"Nucl. Science and Eng. **129**, 149–163 (1998).

[26] W.P. Poenitz and J.W. Meadows, "^{235}U and ^{239}Pu Sample-Mass Determination and Intercomparison,"Argonne National Laboratory Report ANL/NDM-84 (1983).

[27] J. Li, A. Li, C. Rong *et al.*, "Absolute Measurements of ^{235}U and ^{239}Pu Fission Cross Section Induced by 14.7 MeV Neutrons,"Proc. of the Conf. on Nucl. Data for Sci. and Technol., Antwerp 1982, 55–57 (1983).

[28] J.W. Meadows, "The Fission Cross Sections of Some Thorium, Uranium, Neptunium and Plutonium Isotopes Relative to ^{235}U,"Argonne National Laboratory Report ANL/NDM-83 (1983); J.W. Meadows, "The Fission Cross Sections of Plutonium-239 and Plutonium-242 Relative to Uranium-235 from 0.1 to 10 MeV,"Nucl. Science and Eng. **68**, 360–363 (1978).

[29] E. Pfletschinger and F. Käppeler, "A Measurement of the Fission Cross Sections of ^{239}Pu and ^{233}U Relative to ^{235}U,"Nucl. Science and Eng. **40**, 375–382 (1970).

[30] P.H. White J.G. Hodgkinson and G.J. Wall, "Measurement of Fission Cross-Sections for Neutrons of Energies in the Range 40–500 keV,"International Atomic Energy Agency Report STI/PUB/101 **1**, 219–233 (1965).

[31] P.H. White and G.P. Warner, "The Fission Cross Sections of ^{233}U, ^{234}U, ^{236}U, ^{238}U, ^{239}Pu, ^{240}Pu and ^{241}Pu Relative to that of ^{235}U for Neutrons in the Energy Range 1–14 MeV,"J. of Nucl. Energy **21**, 671–679 (1967).

[32] K. Merla, P. Hausch, C.M. Herbach *et al.*, "Absolute Measurements of Neutron Induced Fission Cross-sections of ^{235}U, ^{238}U, ^{237}Np and ^{239}Pu using the Time Correlated Associated Particle Method (TCAPM)," Proc. of Conf. on Nucl. Data for Science and Technol., ed.: Quaim, Springer-Verlag (Heidelberg) (1992), 510–513 (1992); I.D. Alkhazov, L.V. Drapchinsky, V.A. Kalinin *et al.*, "New Results of Absolute Cross-section Measurements for the Heavy Nuclide Fission Induced by Fast Neutrons," Proc. of the Conf. of Nuclear Data for Science and Techn., Mito 1988, 145–148 (1988); R. Alt, W. Grimm, M. Josch *et al.*, "The Application of a Time-correlated Associated Particle Method for Absolute Cross-section Measurements of Heavy Nuclides," Proc. of the Intern. Conf. for Nucl. Cross Sections for Technol. Knoxville 1979, 990–994 (1979).

[33] M. Cance and G. Grenier, "Absolute Neutron Fission Cross Section of ^{235}U, ^{238}U, and ^{239}Pu, at 13.9 and 14.6 MeV," Nucl. Science and Eng. **68**, 197–203 (1978).

[34] I. Szabo, J.L. Leroy and J.P. Marquette ,"Measure Absolute de la Section Efficace de Fission de ^{235}U, de ^{239}Pu et de 241Pu entre 10 keV et 2.6 MeV," Proc. of the Second Conf. on Neutron Physics, Kiev 1973, **3**, 27–45 (1973); I. Szabo and J.P. Marquette ,"Measurement of the Neutron Induced Fission Cross Sections of Uranium 235 and Plutonium 239 in the MeV Energy Range," Proc. of the Meet. on Fast Neutr. Cross Sections of U and Pu, Argonne 1976, 208–222 (1976); I. Szabo, G. Filippi, J.L. Huet *et al.*, "New Absolute Measurement of the Neutron-induced Fission Cross Sections of ^{235}U, ^{239}Pu and ^{241}Pu from 17 keV to 1 MeV," Proc. of the Neutron Standards Symp., Argonne 1970, 257–271 (1970).

[35] W.P. Poenitz, "Measurement of the Ratios of Capture and Fission Neutron Cross Sections of ^{235}U, ^{238}U and ^{239}Pu at 130 to 1400 keV," Nucl. Science and Eng. **40**, 383–388 (1970).

[36] C.A. Uttley and J.A. Phillips, "Fission Cross-Sections of ^{238}U, ^{235}U, ^{233}U, ^{239}Pu and ^{232}Th for 14 MeV Neutrons," United States Atomic Energy Commission Report AERE-NP/R-1996 (1956).

[37] M. Mahdavi, G.F. Knoll and J.C. Robertson, "Measurement of the 14 MeV Fission Cross-Sections for ^{235}U and ^{239}Pu," Proc. of the Conf. on Nucl. Data for Science and Technol., Antwerp 1982, 58–61 (1982).

[38] M.C. Davis, G.F. Knoll, J.C. Robertson *et al.*, "Absolute Measurements of ^{235}U and ^{239}Pu Fission Cross-sections with Photoneutron Sources," Ann. of Nucl. Energy **5**, 569–581 (1978).

[39] B.I. Fursov, V.M. Kupriyanov, V.I. Ivanov *et al.*, "Measurement of the Ratio of the ^{239}Pu and ^{235}U Fission Cross Sections for 0.024–7.4-MeV Neutrons," Soviet Atomic Energy **43**, 894–899 (1977).

[40] M. Várnagy and J. Csikai, "A New Approach to Measuring Fission Cross-section Ratios," Nuclear Instrum. and Methods **96**, 465–468 (1982).

[41] W.D. Allen and A.T.G. Ferguson, "The Fission Cross Sections of ^{233}U, ^{235}U, ^{238}U and ^{239}Pu for Neutrons in the Energy Range 0.030 MeV to 3.0 MeV," Proc. Phys. Soc. A **70**, 573–585 (1957).

[42] J.W. Meadows, "The Fission Cross Sections of ^{230}Th, ^{232}Th, ^{233}U, ^{234}U, ^{236}U, ^{238}U, ^{237}Np, ^{239}Pu, and ^{242}Pu Relative to ^{235}U at 14.74 MeV Neutron Energy," Argonne National Laboratory Report ANL/NDM-97 (1986); J.W. Meadows, "The Fission Cross Section Ratios and Error Analysis for Ten Thorium, Uranium, Neptunium, and Plutonium Isotopes at 14.74 MeV Neutron Energy," Argonne National Laboratory Report ANL/NDM-98 (1987).

[43] X. Zhou, W. Yan, H. Zhuo *et al.*, "Fast Neutron Induced Fission Cross Section for Pu-239," Proc. of the Conf. Nuclear Data for Sci. and Technol., Antwerp 1982, 36–38 (1983).

[44] S. Pommé, "The uncertainty of counting at a defined solid angle," Metrologia **52**, S73–S85 (2015).

[45] S. Pommé, "Methods for primary standardization of activity," Metrologia, **44**, S17–S26 (2007).

[46] C.J. Werner, ed., "MCNP Users Manual - Code Version 6.2," Los Alamos National Laboratory Report LA-UR-17-29981 (2017).

[47] G.W. Carlson, "The Effect of Fragment Anisotropy on Fission-Chamber Efficiency," Nuclear Inst. and Methods **119**, 97–100 (1974).

[48] V.G. Nesterov, Yu.A. Blyumkina and L.A. Kamaeva *et al.*, "Angular Distribution of Fragments from Fission of U^{235} and Pu^{239} by 0.08–1.25 MeV Neutrons," Atomnaya Energiya **16**, 519–521 (1964).

[49] R.B. Leachman and L. Blumberg, "Fragment Anisotropies in Neutron-, Deuteron-, and Alpha-Particle-Induced Fission," Phys. Rev. **137**, B814–B825 (1965).

[50] D. Hensle, "Neutron Induced Fission Fragment Angular Distributions and Momentum Transfer Measured with the NIFFTE Fission Time Projection Chamber", PhD Thesis, Colorado School of Mines (2019); https://mountainscholar.org/handle/11124/173024 .

[51] A.E. Lovell, P. Talou, I. Stetcu *et al.*, "Anisotropies in Neutron-Induced Fission,"in preparation (2020).

[52] G. Coddens, C. Wagemans, A.J. Deruytter *et al.*, "Experimental and Theoretical Investigation of the Backscattering of Fission Fragments," Nucl. Instrum. Methods **66**, 217–228 (1979).

[53] F. Engelkemeir, "Fission-fragment Scattering," Phys. Rev. **146** 304 (1966).

[54] J.P. Biersack and L.G. Haggmark, "A Monte Carlo Computer Program for the Transport of Energetic Ions in Amorphous Targets," Nuclear Inst. and Methods **174**, 257–269 (1980).

[55] J.F. Ziegler, "SRIM-2003," Nuclear Inst. and Methods in Phys. Res. B **219–220**, 1027–1036 (2004).

[56] S. Agostinelli, J. Allison, K. Amako *et al.*, "Geant4—A Simulation Toolkit," Nuclear Inst. and Methods in Phys. Res. A **506**, 250–303 (2003).

[57] C. Budtz-Jorgensen, H.H. Knitter and G. Bortels, "Assaying of Targets for Nuclear Measurements with a Gridded Ionization Chamber," Nuclear Inst. and Methods in Phys. Res. A **236**, 630–640 (1985).

[58] G. Coddens, C. Wagemans and A.J. Deruytter, "Fission Fragment Backscattering Corrections to Absolute Fission Counting Rate Measurements," Nucl. Science and Eng. **74**, 223-224 (1980).

[59] N. Otuka, E. Dupont and V. Semkova, "Towards a More Complete and Accurate Experimental Nuclear Reaction Data Library (EXFOR): International Collaboration Between Nuclear Reaction Data Centres (NRDC)," Nucl. Data Sheets **120**, 272–276 (2014).

[60] K. Kari, "Messung der Spaltquerschnitte von ^{239}Pu und ^{240}Pu relativ zum Spaltquerschnitt von ^{235}U und Streuquerschnitt H (n,p) in dem Neutronenenergiebereich zwischen 0,5–20 MeV,"PhD thesis, Kernforschungszentrum Karlsruhe, GmbH, Karlsruhe, KfK 2673 (1978).

[61] L.W. Weston and J.H. Todd, "Subthreshold Fission Cross Section of ^{240}Pu and the Fission Cross Sections of ^{235}U and ^{239}Pu," Nucl. Science and Eng. **88**, 567–578 (1984).

[62] L.W. Weston and J.H. Todd, "Neutron Fission Cross Sections of ^{239}Pu and ^{240}Pu Relative to ^{235}U," Nucl. Science and Eng. **84**, 248–259 (1983).

[63] C. Wagemans and G. Coddens, "Measurement of the ^{239}Pu(n,f) Cross Section from Thermal up to 30 keV Neutron Energy," Annals of Nucl. Energy **7**, 495–503 (1980).

[64] A.A. Bergman , A.G. Kolosovskiy, A.N. Medvedev *et al.*, "Measurement of the U-233, U-235, Pu-239 Fission Cross Section and its Ratio to U-235 Fission Cross Section in Energy Range from 100 eV until 50 keV,"International Atomic Energy Agency INDC(CCP)-169, 54–57 (1980).

[65] G.W. Carlson and J.W. Behrens, "Measurement of the Fission Cross Sections of Uranium-233 and Plutonium-239 Relative to Uranium-235 from 1 keV to 30 MeV," Nucl. Science and Eng. **66**, 205–212 (1978).

[66] J.L. Perkin, P.H. White, P. Fieldhouse *et al.*, "The Fission Cross Section of ^{233}U, ^{234}U, ^{235}U, ^{236}U, ^{237}Np, ^{239}Pu, ^{240}Pu and ^{241}Pu for 24 keV Neutrons,"J. of Nucl. Energy Paris A/B **19**, 423–437 (1964).

[67] K.D. Zhuravlev, N.I. Kroshkin and L.V. Karin, "Cross Sections for the Fission of ^{235}U AND ^{239}Pu by 2-, 24-, 55-, and 144-keV Neutrons," Sov. J. of Atomic Physics **42**, 62–64 (1977).

[68] I. Garlea, C. Miron, D. Dobrea *et al.*, "Measuring of the Integral Cross-sections at 14 MeV for Reactions ^{115}In(n,n'), ^{197}Au(n,2n), ^{93}Nb(n,2n), ^{27}Al(n,α), ^{56}Fe(n,p), ^{239}Pu(n,f), ^{238}U(n,f), ^{232}Th(n,f) and ^{237}Np(n,f)," Revue Roumaine de Physique, **29**, 421–426 (1984).

[69] W.K. Lehto, "Fission Cross-Section Ratio Measurements of ^{239}Pu and ^{233}U to ^{235}U from 0.24 to 24 keV," Nucl. Science and Eng. **39**, 361–367 (1970).

[70] A. Moat, private communication (1958).

[71] Yu.V. Ryabov, "Measurement of the Fission Cross Section of ^{239}Pu by Neutrons with Energy from 10 eV to 100 keV," Atomnaya Energiya **46**, 154–158 (1979).

[72] R.H. Iyer and R. Sampathkumar, "Total Fission Cross Section Measurements using Solid State Track detectors,"Proc. of the Conf. on Nucl. and Solid State Physics Symp., Roorkee 1969, **2**, 289 (1969).

[73] R. Gwin, E.G. Silver and R.W. Ingle, "Measurement of Neutron Fission Cross Section for ^{239}Pu and ^{235}U from 0.02 eV to 200 keV," Transactions of the American Nucl. Soc. **15**, 481–482 (1972); R. Gwin, E.G. Silver, R.W. Ingle, "Measurement of the Neutron Capture and Fission Cross Sections of ^{239}Pu and ^{235}U, 0.02 eV to 200 keV, the Neutron Capture Cross Sections of ^{197}Au, 10 to 50 keV, and Neutron Fission Cross Sections of ^{233}U, 5 to 200 keV," Nucl. Science and Eng. **59**, 79–105 (1976).

[74] L.W. Weston and J.H. Todd,"Neutron Fission and Absorption Cross-section Measurements for ^{239}Pu and ^{241}Pu," Transactions of the American Nucl. Soc. **15**, 480–481 (1972).

[75] R.E. Coté, M.L. Bollinger, J.M. LeBlanc *et al.*, "Neutron Cross-section Measurements on Plutonium," Bulletin of the American Physical Society **1**, 187 (K5) (1965).

[76] G.D. James, "Cross-sections of the Heavy Nuclei in the Resonance Region,"Proc. of the Conf. on Nucl. Data for Reactors, Helsinki 1970, **1**, 267–286 (1970).

[77] M.G. Schomberg , M.G. Sowerby, D.A. Boyce *et al.*, "Ratio of the Capture and Fission Cross-sections of ^{239}Pu in the Energy Range 100 eV to 30 keV,"Proc. of the Conf. on Nucl. Data for Reactors, Helsinki 1970, **1**, 315–330 (1970).

[78] R. Gwin, L.W. Weston, G. de Saussure *et al.*,"Simultaneous Measurement of the Neutron Fission and Absorption Cross Sections of Plutonium-239 over the Energy Region 0.02 eV to 30 keV," Nucl. Science and Eng. **45**, 25–36 (1971); R. Gwin, L.W. Weston, G. de Saussure *et al.*,"Measurement of the Neutron Fission and Absorption Cross Sections of ^{239}Pu over the Energy Region 0.02 eV to 30 keV, " Nucl. Science and Eng. **40**, 306–316 (1970).

[79] J. Blons, "High Resolution Measurements of Neutron-Induced Fission Cross Sections for ^{233}U, ^{235}U, ^{239}Pu and ^{241}Pu Below 30 keV," Nucl. Science and Eng. **51**, 130–147 (1973).

[80] B. Adams, R. Batchelor and T.S. blue, "The Energy Dependence of the Fission Cross-sections of ^{238}U, ^{235}U and ^{239}Pu for Neutrons in the Energy Range 12.6 to 20 MeV," J. Nuclear Energy A& B **14**, 85–90 (1961).

[81] O. Shcherbakov, A. Donets, A. Evdokimov *et al.*,"Neutron-Induced Fission of ^{233}U, ^{238}U, ^{232}Th, ^{239}Pu, ^{237}Np, $^{\text{nat}}$Pb and ^{209}Bi Relative to ^{235}U in the Energy Range 1–200 MeV," J. of Nucl. Science and Technol. **2**, 230–233 (2002).

[82] L.W. Weston and J.H. Todd, "High-Resolution Fission Cross-Section Measurements of ^{235}U and 239Pu," Nucl. Science and Eng. **111**, 415–421 (1991).

[83] D. Neudecker, "ARIADNE—A Program Estimating Covariances in Detail for Neutron Experiments," Europ. Phys. J. N **4**, 34 (2018).

[84] D. Neudecker, M.C. White, D.E. Vaughan *et al.*, "Validating Nuclear Data Uncertainties Obtained from a Statistical Analysis of Experimental Data with the "Physical Uncertainty Bounds" Method,"Los Alamos National Laboratory Report LA-UR-19-22384, (to be submitted to a journal for publication).

[85] G.M. Hale and M.W. Paris, "Data Covariances from R-Matrix Analyses of Light Nuclei," Nuclear Data Sheets **123**, 165–170 (2015); D.C. Dodder, G.M. Hale and K. Witte, "The Energy Dependent Analysis (EDA) Code,"Los Alamos National Laboratory (unpublished, 1972).

[86] J. Briggs, ed., "International Handbook of Evaluated Criticality Safety Benchmark Experiments (ICSBEP)," Paris: Organization for Economic Co-operation and Development-Nuclear Energy Agency (OECD-NEA) (2016). NEA/NSC/DOC(95)03.

[87] A.C. Kahler, R.E. MacFarlane, R.D. Mosteller *et al.*, "ENDF/B-VII.1 Neutron Cross Section Data Testing with Critical Assembly Benchmarks and Reactor Experiments," Nucl. Data Sheets **112**, 2997–3036 (2011).

[88] C. Wong, J.D. Anderson, P. Brown *et al.*, "Livermore Pulsed Sphere Program: Program Summary through July 1971," Lawrence Livermore Laboratory Report UCRL-ID-51144 (1972).

[89] A.A. Marchetti and G.W. Hedstrom, "New Monte Carlo Simulation of the LLNL Pulsed-Sphere Experiments," Lawrence Livermore Laboratory Report UCRL-ID-131461 (1998).

[90] R.D. Mosteller, S.C. Frankle and P.G. Young, "Data Testing of ENDF/B-VI with MCNP: Critical Experiments, Thermal-reactor Lattices and Time-of-flight Measurements," Los Alamos National Laboratory Report LA-UR-96-2143 (1996).

[91] T. Goorley, "MCNP6.1.1-Beta Release Notes," Los Alamos National Laboratory Report LA-UR-14-24680 (2014).

[92] D.A. Brown, M.B. Chadwick, R. Capote *et al.*, "ENDF/B-VIII.0: The 8th Major Release of the Nuclear Reaction Data Library with CIELO-project Cross Sections, New Standards and Thermal Scattering Data," Nucl. Data Sheets **148**, 1–142 (2018).

[93] T. Kawano, "DeCE: The ENDF-6 data interface and nuclear data evaluation assist code," J. Nuclear Science and Technology, published online on https://doi.org/10.1080/00223131.2019.1637797 (2019).

[94] R.E. MacFarlane, D.W. Muir, R.M. Boicourt *et al.*, "The NJOY Nuclear Data Processing System, Version 2016," Los Alamos National Laboratory Report LA-UR-17-20093 (2017).

[95] O. Cabellos and L. Fiorito, "Examples of Monte Carlo techniques applied for nuclear data uncertainty propagation," EPJ Web of Conferences **211**, 07008 (2018).